4984–5002 *Nucleic Acids Research, 2011, Vol. 39, No. 12* *Published online 4 March 2011*
doi:10.1093/nar/gkr116

Modulation of Dnmt3b function *in vitro* by interactions with Dnmt3L, Dnmt3a and Dnmt3b splice variants

Beth O. Van Emburgh and Keith D. Robertson*

Department of Biochemistry and Molecular Biology, Cancer Research Center, CN-2151, Georgia Health Sciences University, 1410 Laney Walker Blvd., Augusta, GA 30912, USA

Received October 5, 2010; Revised February 9, 2011; Accepted February 15, 2011

ABSTRACT

DNA methylation, an essential regulator of transcription and chromatin structure, is established and maintained by the coordinated action of three DNA methyltransferases: DNMT1, DNMT3A and DNMT3B, and the inactive accessory factor DNMT3L. Disruptions in DNMT3B function are linked to carcinogenesis and genetic disease. DNMT3B is also highly alternatively spliced in a tissue- and disease-specific manner. The impact of intra-DNMT3 interactions and alternative splicing on the function of DNMT3 family members remains unclear. In the present work, we focused on DNMT3B. Using a panel of *in vitro* assays, we examined the consequences of DNMT3B splicing and mutations on its ability to bind DNA, interact with itself and other DNMT3's, and methylate DNA. Our results show that, while the C-terminal catalytic domain is critical for most DNMT3B functions, parts of the N-terminal region, including the PWWP domain, are also important. Alternative splicing and domain deletions also influence DNMT3B's cellular localization. Furthermore, our data reveal the existence of extensive DNMT3B self-interactions that differentially impact on its activity. Finally, we show that catalytically inactive isoforms of DNMT3B are capable of modulating the activity of DNMT3A–DNMT3L complexes. Our studies therefore suggest that seemingly 'inactive' DNMT3B isoforms may influence genomic methylation patterns *in vivo*.

INTRODUCTION

Genome-wide patterns of DNA methylation in mammals are established and maintained by a family of three enzymatically active DNA methyltransferases: DNMT1, DNMT3A and DNMT3B, and a fourth catalytically inactive co-factor, DNMT3L. DNMT3L possesses homology to and stimulates the activity of DNMT3A and DNMT3B. DNMT3L also 'directs' DNA methylation to genomic regions lacking histone H3, lysine 4 (H3K4) trimethylation, a mark associated with transcriptional activity (1,2). DNMT3A, DNMT3B and DNMT3L exist in a complex in pluripotent cells that interacts with the core histones (2,3). DNMT1 is traditionally regarded as the DNMT specialized to carry out maintenance methylation following replication, while DNMT3A/DNMT3B are regarded as the *de novo* enzymes, critical for establishing new DNA methylation patterns during embryonic and germ line development (4). While the exact genomic targets of each DNA methyltransferase have not been systematically defined, there appear to be both overlapping and distinct targets of each DNMT. For example, murine knockout studies revealed a particularly critical role for Dnmt3b in methylating pericentromeric regions. While Dnmt1 was also necessary for methylation of pericentromeric domains, Dnmt3a activity was not (5). In contrast, Dnmt3a and its cofactor Dnmt3L (but not Dnmt3b1), are critical for establishment of maternal methylation imprints during oogenesis (4). Exactly how DNMT3A, DNMT3B and DNMT3L interact and collaborate to methylate the genome remains unknown. Since DNMT3L expression is largely confined to certain developmental periods or germ cell compartments, mechanisms of DNMT3L-independent targeting of DNMT3A and DNMT3B must also exist.

Proper patterns of DNA methylation are essential not only for mammalian embryonic development, but also for normal cellular homeostasis once development is complete. All cancer cells display profound disruptions in DNA methylation patterns in the form of a global reduction in DNA methylation, primarily affecting repetitive DNA sequences, and at the same time, region-specific hypermethylation events at normally unmethylated CpG island promoter regions. Repetitive element hypomethylation contributes to genomic instability while CpG island hypermethylation leads to heritable long-term silencing

*To whom correspondence should be addressed. Tel: +1 706 721 0099; Fax: +1 706 721 2928; Email: krobertson@georgiahealth.edu

of genes critical for regulating cell proliferation, apoptosis and DNA repair (6,7). Overexpression of Dnmt3b, but not Dnmt3a, in the $Apc^{Min/+}$ murine colon cancer model system resulted in increased tumor number, microadenoma size and incidence of tumor suppressor gene hypermethylation events (8) underscoring the importance of properly regulated DNMT levels to cellular growth control. Disruption of DNA methylation patterns during human development also has profound consequences. Approximately two-thirds of immunodeficiency, centromere instability, facial anomalies (ICF) syndrome patients have germ line mutations in the *DNMT3B* gene that are thought to result in at least partial loss of one or more of DNMT3B's functions. ICF syndrome patients display variable defects in B and T cell function, developmental abnormalities, mental retardation and loss of DNA methylation at pericentromeric and centromeric regions (satellite 2/satellite 3 repeats and alpha satellite, respectively), non-satellite repeats, single copy autosomal genes and genes on the inactive X chromosome (6,9–12). While several studies have shown that ICF syndrome-associated *DNMT3B* mutations reduce its catalytic activity and/or its ability to interact with DNMT3L (13,14), much remains unknown as to how partial loss of DNMT3B function leads to the unusual and cell type-specific phenotypes characteristic of ICF patients.

In addition to the important roles for DNMT3B in development and carcinogenesis, it stands out among DNA methyltransferases in the number of alternatively spliced isoforms derived from the *DNMT3B* locus (>40) (15,16). Many alternatively spliced forms of DNMT3B are expressed in a tissue and/or developmental stage-specific manner, such as DNMT3B4/DNMT3B5 in testis (17), and DNMT3B3Δ5, which is associated with pluripotency (18). In tumor cells, normally occurring isoforms, such as DNMT3B4 in hepatocellular carcinoma and DNMT3B3Δ5 in multiple tumor types, become aberrantly overexpressed and contribute to pericentromeric repeat demethylation and genomic instability (18,19). Still other DNMT3B isoforms appear to be largely tumor specific. Ectopic expression of DNMT3B7, the most widely expressed DNMT3B isoform specifically linked to cancer, creates instability in DNA methylation patterns (both hypo- and hypermethylation events) in cell lines and promotes tumorigenesis *in vivo* in an *Eμ-Myc* transgenic mouse lymphoma model (15,20). Interestingly, most of the DNMT3B alternative splicing events, whether normal (e.g. DNMT3B3) or tumor associated (e.g. DNMT3B7), result in isoforms lacking some or all of the C-terminal catalytic domain and are inactive (DNMT3B3) or predicted to be inactive (15,21). Exactly how these isoforms influence other active co-expressed forms of DNMT3B, DNMT3A or DNMT3L remains largely unknown; however, the observation that improper expression of DNMT3B7 results in developmental defects and enhances tumorigenesis (20), demonstrates that regulation of DNMT3B splicing is critically important.

In the present work, we were interested in defining the domains of DNMT3B that are important for its function (here referring to its ability to bind and methylate DNA, and interact with other DNMT3 family members/splice variants), and also in determining how the reported DNMT3B–DNMT3L and DNMT3B–DNMT3A interactions affect these functions. DNMT3B exists in a complex with DNMT3A and DNMT3L and it interacts with itself (2,3,14,20,22–24). One of the most widely expressed splice variants of DNMT3B (DNMT3B3) is catalytically inactive yet co-expressed in cells with other active DNMT3 isoforms. The full extent and functional consequences of intra-DNMT3 interactions remains unclear. Since DNMT3A has been more extensively studied in this context than DNMT3B, we focused our studies on DNMT3B. We expressed and purified a panel of DNMT3B splice variants (human and murine), DNMT3B mutants in which regions of the N- and C-terminal domains were deleted, and ICF-syndrome-associated *DNMT3B* point mutations. All DNMT3B isoforms were tested for their ability to bind DNA and to interact with DNMT3L *in vitro*. Functional studies included analysis of DNA methylation patterns using three independent assays based on: methylation-sensitive restriction enzyme digestion, bisulfite genomic sequencing (BGS) and bisulfite pyrosequencing. We also examined the effect of different DNMT3B isoforms on the activity of DNMT3A–DNMT3L complexes as they would be expected to occur in a native complex in ES cells (2), and on their cellular localization properties and ability to co-localize with other Dnmt3s. Our *in vitro* data reveal the existence of extensive interactions among DNMT3 family members that are capable of modulating a number of their functional properties. In addition, our results demonstrate that DNMT3B isoforms lacking activity, because of alternative splicing or mutation, are capable of altering the activity of complexes containing enzymatically active DNMT3 isoforms, suggesting that they contribute to regulating genomic methylation patterns *in vivo*.

MATERIALS AND METHODS

Electrophoretic mobility shift assay

Recombinant proteins (preparation described in the Supplementary Data) were used to analyze protein–DNA interactions with a satellite 2 DNA probe and quantitated as described previously (18). Briefly, bands corresponding to bound and unbound probe were quantitated using Quantity One 4.6.1 software (BioRad) to calculate the sum of the intensity of the bands in each lane. The percent shift curves were fit and K_D values were derived using the three parameter Hill equation [$y = ax^b/(c^b + x^b)$] in Sigma Plot 8.0. All electrophoretic mobility shift assays (EMSAs) were repeated at least twice. Most EMSA reactions were performed using recombinant DNMTs in the 0–700 nM range. Proteins or protein mixtures displaying particularly high DNA binding affinity were repeated using a 0–200 nM concentration range (in 20 nM increments). Linear to saturated binding in these protein concentration ranges was determined empirically in early experiments (not shown). When proteins were combined, they were used in equimolar amounts. Statistical significance was determined using a two-sample *t*-test (NCSS 2001).

GST pull down and western blotting

Protein–protein interactions were examined using purified recombinant GST-tagged Dnmt3L, Dnmt3b1-C-terminal domain (CD), Dnmt3b3-CD and GST bound to glutathione sepharose resin (as a negative control, preparation of proteins is described in the Supplementary Data). Recombinant 6XHis-tagged proteins (0.05 nmol) were incubated with 2.5–10 µl of resin-bound protein (0.6 µg) and, if needed to equalize total resin volume, BSA blocked empty resin, in either low salt (100 mM KCl) or high salt (150 mM KCl) pull down buffer [25 mM HEPES (pH 7.9), 12.5 mM $MgCl_2$, l00 or 150 mM KCl, 10% glycerol, 0.1% NP-40] for 1.5 h. Beads were washed 4× for 10 min each. After washing, beads were mixed with an equal volume of 2× protein loading dye and resolved on an 8% SDS–PAGE gel. Proteins were transferred overnight to PVDF membrane. Protein interactions with GST fusion proteins were detected by western blotting with anti-6XHis antibody [His-probe (H-15): SC-803, Santa Cruz or monoclonal anti-His: G020, ABM, 1:1000 dilution] as described previously (18). Films with pull down and input were scanned and the composite images shown generated without further computerized image adjustment (e.g. alterations in contrast, brightness, etc.).

DNA methyltransferase activity assays

Activity assay conditions, adapted from Takeshima *et al.* (25), were 20 mM Tris (pH 7.4), 5 mM EDTA, 25 mM NaCl, 10% glycerol, 200 µM DTT, 80 µM *S*-adenosyl-L-methionine (SAM, New England Biolabs) and 1.5 µg pSL301 plasmid containing the SAT2 sequence. The reaction mixture was incubated at 37°C for 7 h, with fresh SAM added after the first 4 h. For reactions comparing enzyme activity with and without Dnmt3L, 0.15 nmol of each purified methyltransferase was mixed in equimolar concentrations. For reactions combining Dnmt3b's with Dnmt3a and Dnmt3L, 0.06 nmol of each purified methyltransferase was used. A negative control (an active methyltransferase but no SAM) was also included in all reactions. For restriction enzyme digestion analysis, 0.5 µg of plasmid from the assay mixture was removed and digested with 400 µg/ml proteinase K at 55°C for 10 min. The digest was extracted once with phenol:chloroform:iso-amyl alcohol and ethanol precipitated. The precipitated DNA was digested with 5 U of HpaII overnight and analyzed on a 1.5% agarose gel stained with ethidium bromide. Gels were visualized using a Bio-Rad gel documentation system and bands were quantitated using Quantity One software (v4.6.1, Bio-Rad). The relative quantity of higher molecular weight bands that resulted from methylation-mediated inhibition of HpaII digestion was calculated as a percentage using the sum of the intensity of the bands in each lane.

BGS and pyrosequencing

Following the methyltransferase activity assay, 0.5 µg of plasmid was digested with 10 U of *Pvu*II (to linearize) in preparation for bisulfite modification. Bisulfite modification was performed essentially as described (12). An additional denaturation step, heating at 95°C for 10 min, was included prior to addition of sodium hydroxide. Modified plasmid DNA was then used as a template for BGS and pyrosequencing. BGS PCR products were gel purified using the Qiaex II Gel Extraction Kit (Qiagen). PCR products were then cloned using the TOPO TA Cloning Kit (Invitrogen). At least 10 clones were sequenced for each PCR product using the M13 reverse primer. All sequencing was completed by the Interdisciplinary Center for Biotechnology Research at the University of Florida. Sequence data was analyzed and figures generated using the web-based Quantification Tool for Methylation Analysis (QUMA) software (26). Processivity analyses were completed by calculating the processivity indices using the BGS data as in ref. (27) where an index of 1 indicates that all CpGs in the clone are methylated and 0 indicates that no contiguous CpGs are methylated. Only clones exhibiting methylated CpG sites could be scored. Significance was calculated using the Wilcoxon rank-sum test (NCSS, 2001). For pyrosequencing, the forward primers were the same as for BGS and the reverse primers were biotinylated at the 5′-end (Supplementary Table S1). Pyrosequencing PCR products (10–15 µl) were used with PyroMark Gold Q96 Reagents on a PyroMark MD Pyrosequencer (Qiagen) following the manufacturer's protocol and as described previously (28). Background was subtracted using the inactive/negative controls, which were included in all pyrosequencing runs.

Transfections and microscopy

HEK 293T cells (American Type Culture Collection) were cultured in McCoy's-5A media supplemented with 10% heat inactivated fetal bovine serum and 2 mM L-glutamine. Cells were plated at 10^5/ml on 25 mm diameter cover slips in six-well tissue culture dishes. After 48 h, cells were transfected with 2 µg of each expression construct using Lipofectamine 2000 transfection reagent according to the manufacturer's protocol (Invitrogen). Twenty-four hours after transfection, cells were fixed in 2% paraformaldehyde in 1× PBS. DNA was counterstained with 1 µg/ml bisBenzimide H33342 trihydrochloride (Sigma-Aldrich) in 1× PBS and coverslips were mounted onto glass slides with Fluoromount-G (Southern Biotech). Cells were visualized and photographed using a Zeiss LSM 510 META confocal microscope.

RESULTS

In vitro systems for studying Dnmt3b function

The domains responsible for the Dnmt3a–Dnmt3a and Dnmt3a–Dnmt3L interactions, as well as Dnmt3a enzymatic activity, have been much more extensively studied than those of Dnmt3b (1,13,23,29), likely because Dnmt3b displays the lowest catalytic activity among DNMT family members *in vitro*. In addition, an ever growing number of Dnmt3b splice variants are being identified (15,18) and their effect on Dnmt3b in isolation and on other Dnmt3b variants, Dnmt3a and Dnmt3L, are largely unknown. To begin to address these issues we

developed a panel of Dnmt3b splice variants, constructs in which we deleted regions of the N- and C-terminal domain [including the known PWWP motif that contributes to Dnmt3b DNA and heterochromatin binding (30,31), and the PHD domain, which may mediate interactions between Dnmt3b and other chromatin modifiers (32)], and a panel of ICF syndrome-associated Dnmt3b mutants that were expressed and purified as hexahistidine-tagged (6XHis) fusions from baculovirus infection of Sf9 insect cells or as glutathione-*S*-transferase (GST) fusion proteins from *Escherichia coli* (Figure 1A and B). To study the functional effects of these mutations on Dnmt3b, we employed a panel of assays to measure protein–DNA interaction (EMSA), enzymatic activity (using three assays: methylation-sensitive restriction enzyme digestion, BGS and bisulfite pyrosequencing), and protein–protein interactions using GST pull downs (Figure 1C). The substrate used for the DNA binding and enzymatic activity assays is a plasmid containing a 392 bp fragment of human satellite 2 (SAT2) repeat derived from chromosome 1. Methylation of the entire plasmid (3656 bp) was assessed by digestion with the CpG methylation-sensitive restriction enzyme HpaII and smaller regions of the plasmid backbone and SAT2 insert were analyzed at high resolution using BGS and/or pyrosequencing (Figure 1D). SAT2 is a well established, CpG-rich, native DNMT3B target sequence *in vivo* (5,24). A comparably CpG-rich region of the plasmid backbone was used as a comparison to SAT2 for most assays to determine if particular effects were sequence specific. Effects were monitored using *in vitro* assays so that all aspects of the reactions (proteins, substrates, conditions and stoichiometry) could be experimentally defined and easily manipulated.

Effect of Dnmt3b alternative splicing on protein–DNA interactions, interaction with Dnmt3L, and enzyme activity

To begin to examine the functional consequences of Dnmt3b alternative splicing, we expressed and purified murine and human Dnmt3b1, the full-length enzyme expressed largely in ES cells (16), murine Dnmt3b2 and murine/human Dnmt3b3. Dnmt3b3 is among the most widely expressed Dnmt3b splice variants in somatic cells (16,17). Murine Dnmt3a was used as a reference to compare its properties to those of Dnmt3b using the same panel of *in vitro* assays. Effects of alternative splicing on Dnmt3b DNA binding were assessed by EMSA using a 461-bp fragment containing human SAT2 (18). Increasing concentrations of purified recombinant Dnmt3 (0–700 nM) were added to a fixed concentration of SAT2 DNA probe, DNA–protein complexes were resolved on agarose gels and visualized using SYBR green staining, and binding affinities determined using the Hill equation, as we have done previously (18). Representative EMSA gels are shown in the top portion of Figure 2A. Dnmt3b1 displayed the highest DNA binding affinity among the isoforms tested (K_D = 183 nM, Table 1). Exclusion of exon 11 (Dnmt3b2) reduced DNA binding affinity and exclusion of exons 11, 22 and 23 (Dnmt3b3 isoform) further reduced binding affinity (K_D = 293 nM). The DNA binding affinities of human DNMT3B1 and DNMT3B3 (lacking exons 10, 21 and 22) were almost identical to their murine homologs. The binding affinity of Dnmt3a for SAT2 was the highest of all Dnmt3 isoforms tested (Figure 2A and Table 1). Quantitation data fit to the Hill equation for all Dnmt3s is shown in the lower panel of Figure 2A and all K_D values derived from these plots are summarized in Table 1.

Consequences of alternative splicing on Dnmt3b's ability to interact with Dnmt3L were then examined using GST pull downs. Buffers of low and moderate stringency (defined by KCl concentration) were employed to obtain an estimate of interaction strength. While all murine and human Dnmt3b isoforms interacted strongly with GST-Dnmt3L under lower stringency conditions (except the Δ671–859 mutant), the Dnmt3L–Dnmt3b2 and Dnmt3L–Dnmt3b3 interactions were lost under the moderate stringency pull down conditions (Figure 2B, Table 1), suggesting that these alternatively spliced regions contribute to the Dnmt3L–Dnmt3b interaction. Identical results were obtained with human DNMT3B1 and DNMT3B3. Loading control westerns for both the 6XHis- and GST-tagged proteins, which were set-up in an identical manner to and western blotted with the pull downs (lower panels of Figure 2B) demonstrate that samples are comparably loaded. Using baculovirus/Sf9-derived 6XHis-tagged Dnmt3L in a pull down reaction with GST-Dnmt3L, we found no evidence that Dnmt3L interacts with itself (data not shown). While it is well established that Dnmt3L stimulates the activity of Dnmt3a and Dnmt3b and enhances Dnmt3a cofactor SAM binding, Dnmt3L did not appear to alter Dnmt3a's DNA binding affinity in a previous study (1). When DNMT3B1 was mixed with GST-Dnmt3L we observed significant enhancement of DNA binding affinity compared to addition of equivalent amounts of GST (Figure 2A) demonstrating that, at least for DNMT3B1 and SAT2 under our reaction conditions, Dnmt3L is capable of modulating the DNA binding affinity of DNMT3B. Dnmt3L alone did not bind SAT2 in the protein concentration range we employed (data not shown). DNMT3B3–Dnmt3L complexes did not resolve sufficiently on the EMSA gels preventing us from determining if Dnmt3L also enhanced the binding of this Dnmt3b splice variant (data not shown). Effects of Dnmt3b alternative splicing on its interaction with Dnmt3L are summarized in Table 1.

We next analyzed the effect of alternative splicing on Dnmt3b enzymatic activity using three different methods. In the first assay, the 3656 bp SAT2-containing plasmid was used as a substrate for *in vitro* methylation reactions (Figure 1D). Following a 7 h incubation of enzyme with DNA and SAM, protein was removed by phenol extraction/ethanol precipitation and the plasmid DNA was digested with HpaII, which only cuts the sequence 5′-C<u>CG</u>G-3′ if the internal cytosine is unmethylated. While lower resolution, this assay allows for analysis of a large number of CpG sites over the entire plasmid. As expected, human and murine Dnmt3b1 and Dnmt3b2 were active on their own, albeit at low levels, and were stimulated ~2–7-fold by the addition of an equimolar

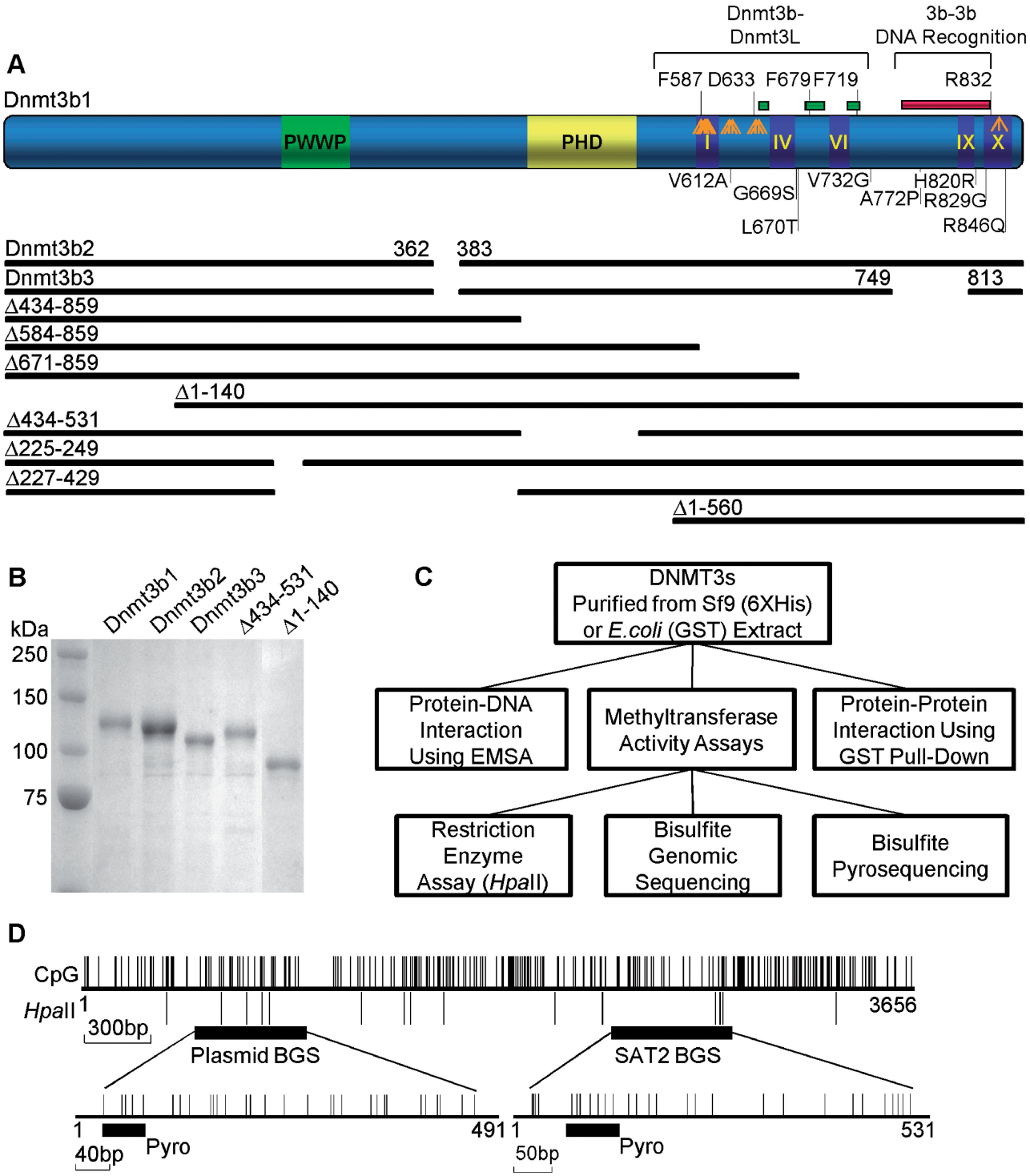

Figure 1. Assay systems, constructs and DNA templates used to assess Dnmt3b functions *in vitro*. (**A**) Schematic representation of Dnmt3b1 and the splice variants/deletions expressed and purified for *in vitro* studies. Critical domains and catalytic motifs are highlighted. SAM interaction sites are indicated by orange arrows. Numbers represent the amino acids of murine Dnmt3b1. Amino acids listed below represent ICF syndrome-associated mutations introduced into the murine sequence at homologous positions to human DNMT3B1 (Supplementary Table S2). Amino acids and red/green bars above Dnmt3b1 represent regions predicted to be important for protein–protein interaction based on Dnmt3a–Dnmt3L structural studies (29). (**B**) Representative coomassie blue stained gel showing a subset of the *in vitro* expressed purified 6XHis-tagged recombinant proteins used in this study. (**C**) Box chart of methodology employed to analyze functional effects of splice variants/deletions/ICF mutations. (**D**) Plot of CpG and HpaII sites in the plasmid containing the satellite 2 (SAT2) sequence used as the template DNA for *in vitro* activity and protein–DNA interaction assays. CpG sites analyzed by bisulfite genomic sequencing (BGS) and pyrosequencing (denoted by thick horizontal lines) are enlarged and shown below.

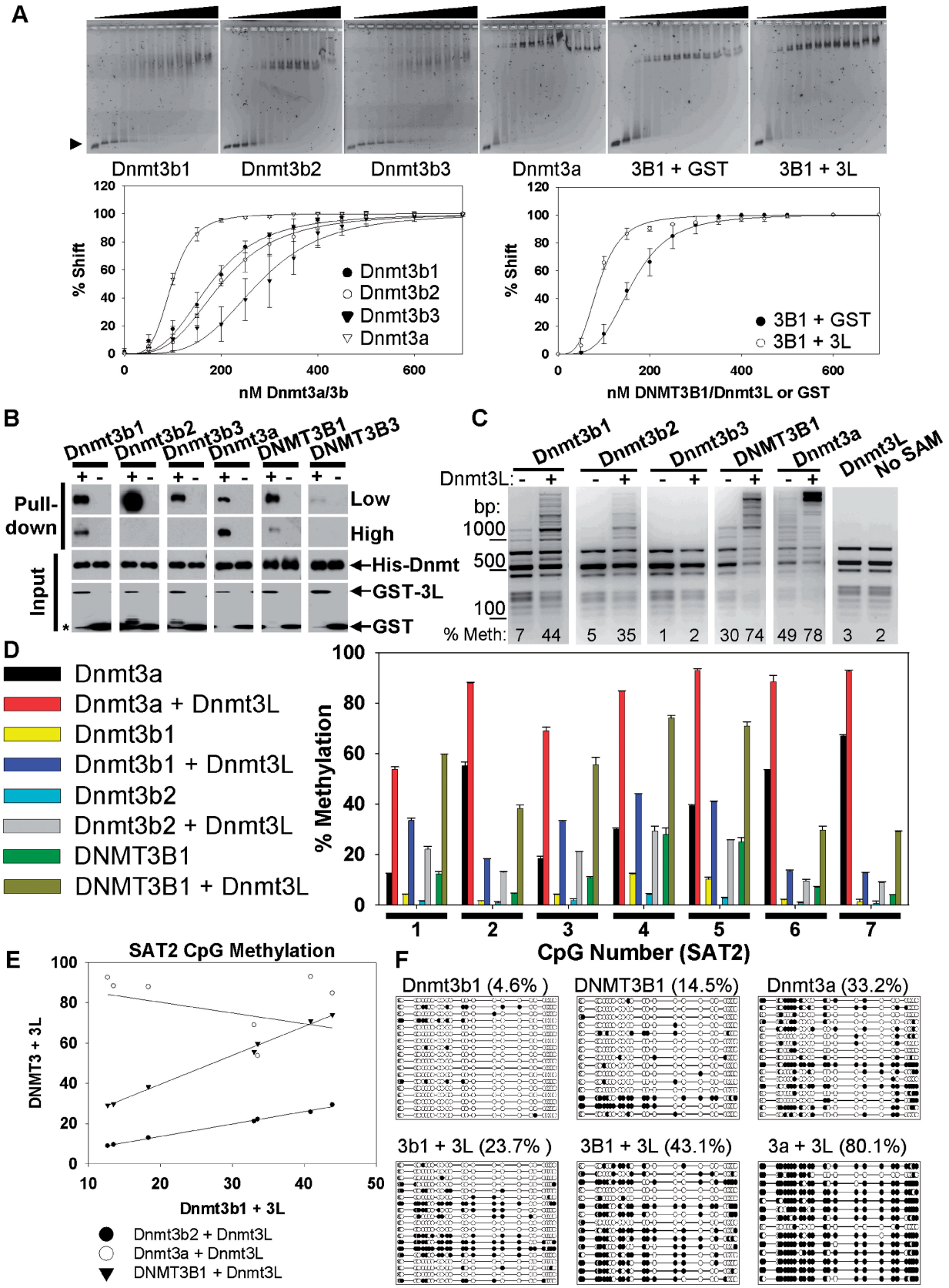

Figure 2. Functional effects of Dnmt3b alternative splicing on protein–DNA binding, interaction with Dnmt3L, and enzyme activity. (**A**) Top panel: representative SYBR green stained EMSA gels with increasing amounts of the Dnmt3 proteins indicated (0–700 nM). Arrowhead—free probe. Bottom panels: percent shift quantitated from EMSA gels. Curves were fit using the Hill equation. Left: Dnmt3b's and Dnmt3a. Right: effect of Dnmt3L (or GST) on DNMT3B1 binding to DNA. (**B**) GST pull down analysis of protein–protein interactions between the indicated Dnmt3

Continued

amount of Dnmt3L to the reactions (Figure 2C). Dnmt3a displayed the highest level of enzymatic activity on its own and Dnmt3b3 was completely inactive with and without Dnmt3L.

To examine DNA methylation quantitatively at single CpG resolution and to determine if site preferences exist, we used bisulfite pyrosequencing. While pyrosequencing is limited to a relatively small region (~50 bp), it is highly quantitative, provides single CpG site resolution, and is amenable to test a large number of reaction conditions (33). A 49-bp region (with five CpG sites) of the plasmid backbone and a 68-bp region (containing seven CpG sites) of the SAT2 insert were analyzed by pyrosequencing (Figure 1D). In keeping with the previous analysis, all Dnmt3 isoforms displaying enzymatic activity in the HpaII assay also demonstrated activity on the SAT2 insert (Figure 2D) and the plasmid backbone (Supplementary Figure S1A). Data are presented as the percent methylation at each CpG site in the analyzed region (Figure 2D and Supplementary Figure S1A) and as a total percent methylation averaged across all sites (Table 1). Interestingly, while Dnmt3L addition stimulated methylation at all sites to some extent (~3–5-fold for human/murine Dnmt3b1), there were some marked differences in the ability of Dnmt3b to methylate certain CpG sites. For example, CpGs 2, 6 and 7 in the SAT2 pyrosequencing region were less well methylated by Dnmt3b1 than the remaining CpG sites, and, interestingly, these three sites were among the most highly methylated by Dnmt3a (Figure 2D). Addition of Dnmt3L preferentially increased methylation at CpG sites less preferred by Dnmt3b (or Dnmt3a) alone (Figure 2D, Supplementary Figure S1A). Dnmt3L-mediated increases in Dnmt3a and Dnmt3b1 activity on SAT2 were not linear across each CpG site, but rather exhibited a hyperbolic correlation as the fold change was greatest at sites of low methylation and decreased at sites with high methylation (Supplementary Figure S1B). This trend, however, was not visible with Dnmt3b1 on the plasmid sequence as the three CpGs with the lowest methylation showed no increase, or even decreased methylation, when Dnmt3L was present in the reaction (Supplementary Figure S1B). While there was a strong correlation between sites methylated by each active Dnmt3b isoform in the presence of Dnmt3L (e.g. Dnmt3b1 + Dnmt3L versus Dnmt3b2+ Dnmt3L), there was no correlation between CpG sites methylated by Dnmt3b compared to Dnmt3a (both in the presence of Dnmt3L), indicating that these two enzymes have distinct site preferences (Figure 2E, Supplementary Figure S1B). In addition, while the activity of Dnmt3b2 on its own was lower than that of Dnmt3b1 at all CpG sites, addition of Dnmt3L increased Dnmt3b2 activity substantially (~10–58-fold for SAT2 and plasmid regions) such that the total level of methylation resulting from the Dnmt3b2+Dnmt3L reaction was almost the same as that in the Dnmt3b1+Dnmt3L reaction (Figure 2D, Table 1). Therefore the Dnmt3b2 splice variant does not alter sequence preference. Although human DNMT3B1 generally had greater activity than murine Dnmt3b1, the overall pattern (or preference) of CpG site methylation of the human and murine enzymes was very similar (Figure 2D and E, Supplementary Figure S1A and B).

Finally, for many of the catalytically active Dnmt3b isoforms (3b1/3b2), we analyzed DNA methylation patterns over the entire 531 bp SAT2 insert (28 CpG sites) and a roughly equivalent sized region of the plasmid backbone (491 bp, 30 CpGs) as a comparison, using traditional BGS. Results for the single clone-based analysis (summarized in Figure 2F, Supplementary Figure S1C and D and Table 1) are generally very comparable to the data derived from pyrosequencing. All Dnmt3b constructs possessed low to moderate activity on their own and were stimulated by addition of Dnmt3L. As for the pyrosequencing experiments, Dnmt3b2 displayed lower activity than Dnmt3b1 on SAT2, but Dnmt3b2 was stimulated to a much greater extent by Dnmt3L than Dnmt3b1 was (Table 1). Results with the plasmid sequence differ to some extent from SAT2 in that Dnmt3b1 and Dnmt3b2 are more similar in their activity levels, suggesting that Dnmt3b activity and Dnmt3L stimulation may, to some extent, be context specific. By analyzing patterns of DNA methylation across each clone, we also determined that human and murine Dnmt3b1 methylated both substrates in a processive manner, consistent with an earlier study (13). Interestingly, addition of Dnmt3L to the reactions significantly increased Dnmt3b processivity (Supplementary Figure S1E). Although Dnmt3b2 showed a similar trend in processivity, this did not reach significance because of its lower methylation activity. Thus, like Dnmt3a (34), Dnmt3L acts as a processivity factor for Dnmt3b as well; increasing Dnmt3b methylation at all CpG sites to some extent (Supplementary Figure S1B). Finally, we interrogated our BGS data for the presence of non-CpG methylation, which was recently shown to be much more common than previously thought, at least in stem cells (35). *In vitro* methylation reactions revealed the presence of low

Figure 2. Continued
constructs and GST-Dnmt3L. Western blotting with anti-His antibody was used to detect interactions. +: pull down with GST-Dnmt3L, –: pull down with GST, low and high refer to the 100 and 150 mM KCl used in binding reaction/washes, respectively. The 6X-His fusion protein and GST-fusion protein loading inputs for each reaction are shown below the pull downs to illustrate equal loading. Reactions identical to the pull downs, without washing, were run along with all pull down reactions and proteins detected by western blotting with antibodies against the 6XHis or GST tags. Arrowhead—specific protein, asterisk—non-specific band. (**C**) Representative HpaII restriction digests of SAT2-containing plasmid following the methyltransferase activity assay. –, Dnmt3 enzyme alone; +, Dnmt3 and Dnmt3L. Numbers below indicate percentage methylation quantified from changes in band patterns resulting from inhibition of HpaII cutting due to methylation. (**D**) Methylation of individual CpG sites in SAT2 (Figure 1) by Dnmt3s with and without Dnmt3L analyzed by pyrosequencing. Error bars indicate standard deviation. (**E**) Linear correlation of methylation of individual CpGs between Dnmt3b1 with Dnmt3L and the other indicated Dnmt3s with Dnmt3L using SAT2 pyrosequencing data. Dnmt3b2 and Dnmt3L R: 1, R^2: 1; Dnmt3a and Dnmt3L R: 0.61, R^2: 0.37; DNMT3B1 and Dnmt3L R: 1, R^2: 1. (**F**) SAT2 BGS results for Dnmt3s with and without Dnmt3L. Overall percentage methylation is indicated in parentheses. White circles: unmethylated CpG, black circles: methylated CpG. Each row represents one sequenced clone.

Table 1. Summary of effects of alternative splicing, deletions, and mutations on DNMT3B's functional properties *in vitro*

	Interaction with Dnmt3L	Interaction with Dnmt3b1	Interaction with Dnmt3b3	DNA binding affinity (nM)	Percentage methylation BGS SAT2			Percentage methylation BGS plasmid			Percentage methylation pyrosequencing SAT2			Percentage methylation pyrosequencing plasmid			HpaII digest percentage increase: Dnmt3a and Dnmt3L trimolecular
				Alone	Alone	Dnmt3L	Fold change	Alone	Dnmt3L	Fold change	Alone	Dnmt3L	Fold change	Alone	Dnmt3L	Fold change	
Dnmt3b splice variants																	
Dnmt3b1	++	+	++	183	4.6	23.7**[a]	5.15	0.9	16.8**	18.67	5.11	27.98**	5.48	9.61	15.09	1.57	23.5
Dnmt3b2	+	–	+	205	0.3	23.1**	77.00	1.1	9**	8.18	1.77	18.55**	10.51	0.22	12.94**	58.82	17.2
Dnmt3b3	+	+	++	293**[b]	ND	ND	ND	ND	ND	ND	1.63	1.28	NC	0.54	0.00	NC	27.0
DNMT3B1	++	+	++	163	14.5	43.1**	2.97	7.3	32**	4.38	13.07	51.05**	3.90	7.64	20.50**	2.69	36.8
DNMT3B3	+	+	++	246**	ND	ND	ND	ND	ND	ND	1.49	0.34	NC	0.19	0.13	NC	ND
Dnmt3a	++	++	++	98**	33.2	80.1**	2.41	22.9	62.7**	2.74	39.36	81.36**	2.07	37.21	66.53**	1.79	ND
Dnmt3b1 deletions																	
Δ584–859	+	–	++	239**	ND	ND	ND	ND	ND	ND	ND	ND	ND	ND	ND	ND	27.7
Δ671–859	–	–	++	ND	ND	ND	ND	ND	ND	ND	0.02	0.16	NC	0.21	0.08	NC	2.6
Δ1–140	++	–	+	126	3.6	6.1	1.69	0.6	6.4*	10.67	3.11	16.79**	5.41	1.03	12.75**	12.44	29.6
Δ434–531 (PHD)	++	+	++	217**	ND	12.3	NC	ND	7.8	NC	0.57	13.76**	24.35	6.21	14.51*	2.34	24.1
Δ225–249 (PWWP)	+	–	+	ND	ND	ND	ND	ND	ND	ND	4.56	10.23**	2.25	2.35	4.77*	2.03	8.0
Δ227–429	+	+	++	ND	ND	ND	ND	ND	ND	ND	1.28	3.93**	3.08	1.40	2.52	1.79	2.6
Δ1–560	++	ND	ND	641*	ND	ND	ND	ND	ND	ND	0.96	3.12	3.25	2.30	9.78*	4.25	−2.8
C657A	++	–	–	129**	0.3	ND	NC	0.6	ND	NC	0.37	0.00	NC	0.44	0.03	NC	13.7
ICF syndrome mutations																	
V612A	+	–	+	269**	ND	ND	ND	ND	ND	ND	4.80	0.83**	0.17	0.00	0.00	NC	27.1
G669S	++	+	++	231*	ND	2.5	NC	ND	1.7	NC	2.30	3.94**	1.71	0.09	3.13	35.71	38.2
L670T	+	+	+	248**	ND	ND	ND	ND	ND	ND	0.77	1.21	NC	0.01	0.00	NC	35.8
V732G	+	+	++	233**	ND	ND	ND	ND	ND	ND	0.65	1.71	NC	0.21	0.00	NC	21.4
A772P	+	+	+	219	ND	ND	ND	ND	ND	ND	0.00	1.30	NC	0.43	0.00	NC	32.6
H820R	+	+	+	297	ND	ND	ND	ND	ND	ND	0.95	0.42	NC	0.82	0.63	NC	40.4
R829G	+	–	++	294**	1.6	8.2	5.1	0.3	6.1	20.33	1.86	4.76**	2.55	1.64	4.80**	2.94	22.6
R846Q	+	+	++	303**	0.9	5.4	6.0	0.0	10.3**	NC	1.82	12.69**	6.99	1.93	10.07**	5.22	29.4

[a]*$P < 0.05$, **$P < 0.01$ alone compared to Dnmt3a/3b with Dnmt3L.
[b]*$P < 0.05$, **$P < 0.01$ compared to Dnmt3b1 of same species.
'–', no interaction; '+', interaction at 100 mM KCl only; '++', interaction at 100 and 150 mM KCl; NC, Not calculated (for pyrosequencing if one value was <1.5%); ND, Not done.

but significant non-CpG methylation with a preferred context of CA>CT>CC (Supplementary Figure S1F), supporting the notion that the Dnmt3′s may be primarily responsible for non-CpG methylation *in vivo* in cell types where they are highly expressed, such as stem cells. Taken together, our analysis of three common Dnmt3b isoforms reveals that alternative splicing results in changes in the ability of Dnmt3b to bind DNA, to interact with Dnmt3L, and to catalyze DNA methylation.

Effects of Dnmt3b1 domain deletions on enzyme–DNA interactions, interaction with Dnmt3L, and enzyme activity

We next analyzed the role of different regions of the Dnmt3b N- and C-terminal domains in regulating its function. Given the similar properties of human and murine Dnmt3b1 and Dnmt3b3 in our previous assays, we performed subsequent studies using only murine forms of Dnmt3b. The N-terminal region of Dnmt3b has at least one, relatively non-specific, DNA binding domain, the PWWP region (30). In our assays, the entire Dnmt3b N-terminal domain (amino acids 1–583) bound to the SAT2 DNA probe with moderate affinity (K_D = 239 nM, Figure 3A and Table 1). Deletion of the extreme N-terminal region of Dnmt3b in the context of the full-length protein resulted in a small increase in DNA affinity, while deletion of the PHD domain reduced affinity for SAT2 relative to FL Dnmt3b1. Interestingly, a smaller fragment of the Dnmt3b1 N-terminus encompassing amino acids 1–433, bound SAT2 with high affinity (K_D = 45 nM, Supplementary Figure S2A) suggesting the existence of a strong DNA binding domain in this region. The relevance of this region in the context of full-length Dnmt3b1 is unclear but could become important in C-terminally truncated cancer-specific splice variants (15,21). The isolated C-terminal catalytic domain of Dnmt3b1 also bound DNA, consistent with it retaining activity, but with greatly reduced affinity (Figure 3A and Table 1).

Interaction of Dnmt3b deletion mutants with Dnmt3L was assessed using GST pull down. All deletions and a

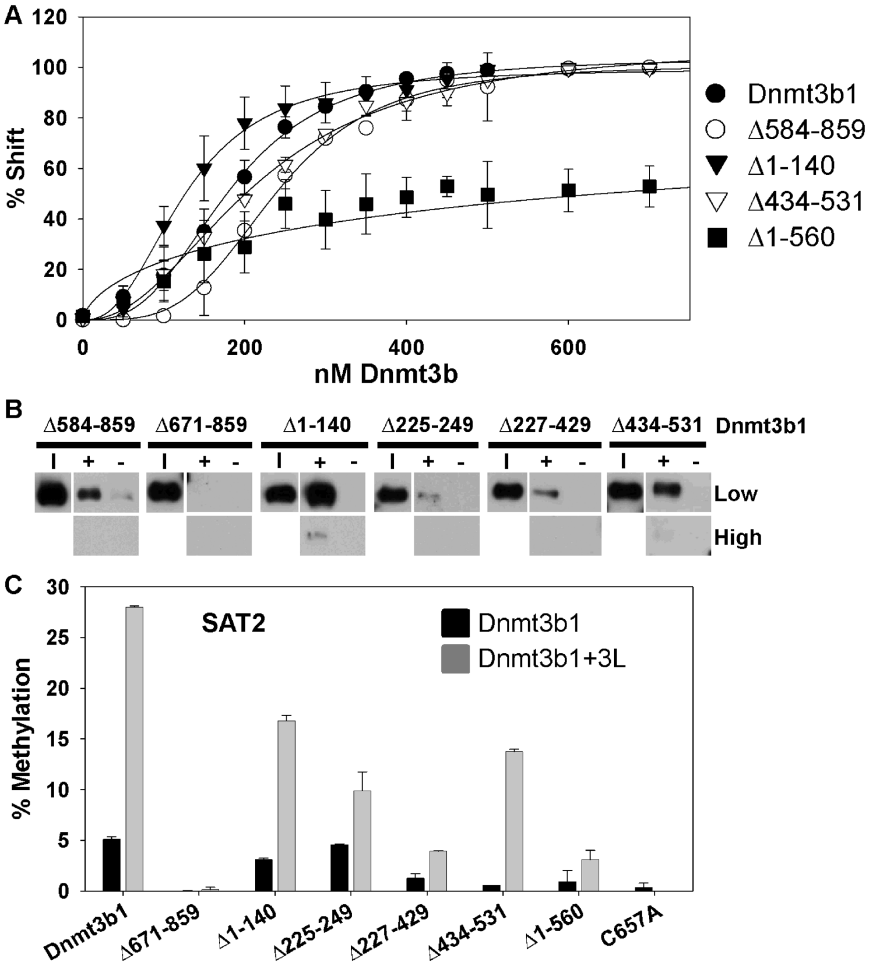

Figure 3. Functional effects of Dnmt3b1 domain deletions on enzyme–DNA binding, interaction with Dnmt3L, and enzymatic activity. (**A**) Quantification of percent shifts from EMSA gels (not shown) as described in Figure 2A using the SAT2 DNA probe. (**B**) Western blot detection of protein–protein interactions between Dnmt3b1 deletions and GST-Dnmt3L following GST pull down analysis under low and moderate stringency conditions (100 and 150 mM KCl, respectively). Symbols are as described in Figure 2B. Input (I) represents the loading of each 6X-His fusion bait protein and is the same for low and high pull downs. (**C**) Overall methylation of the SAT2 sequence by Dnmt3b1 deletions and the Dnmt3b1 C657A catalytic mutant with and without Dnmt3L determined using pyrosequencing.

catalytic site point mutant Dnmt3b1 (C657A) retained some ability to interact with Dnmt3L, with the exception of the Δ671–859 construct. Thus, in the presence of the N-terminus, sequences between amino acids 584 and 671 (including motif I), appear to negatively impact Dnmt3b–Dnmt3L interaction. In contrast, a previous study using the isolated C-terminal domain of Dnmt3b reported that motif I appeared essential for Dnmt3b–Dnmt3L interaction (23). The differing results may be due to our use of the FL form of Dnmt3b or, alternatively, may indicate a defect in the folding of our recombinant Δ671–859 protein. While the C-terminal domain of Dnmt3b is sufficient to interact with Dnmt3L, regions of the N-terminus also play a role in this interaction since deletion of the PWWP domain and flanking sequences (e.g. Δ225–249 mutant) reduced the strength of the Dnmt3b–Dnmt3L interaction (Figure 3B and Table 1).

Pyrosequencing DNA methylation analysis of SAT2 and plasmid regions revealed that, while the isolated catalytic domain of Dnmt3b1 is active and capable of being stimulated by Dnmt3L, as reported previously (36), its activity is greatly reduced compared to the full-length form (Figure 3C and Supplementary Figure S2B). The C657A mutant was completely inactive (by both pyrosequencing and BGS, Figure 3C and Supplementary Figure S2B–D), demonstrating the existence of only one catalytic center in Dnmt3b. Like the interaction between Dnmt3b and Dnmt3L, the N-terminal region also influenced catalytic activity. For example, deletion of the PWWP domain and flanking sequences (e.g. Δ227–429) dramatically reduced activity, while deletion of the PHD domain or the extreme N-terminus of Dnmt3b resulted in more mild changes in activity (Figures 3C, Supplementary Figure S2B and Table 1). The reduced ability of Dnmt3L to stimulate the activity of mutants such as Δ227–429, particularly on SAT2, is in keeping with their impaired ability to interact with Dnmt3L (Figure 3B). BGS data of Dnmt3b1 mutants that retained detectable activity was consistent with the pyrosequencing data and also revealed that none of the domain deletions altered Dnmt3b's CpG site preference in the presence or absence of Dnmt3L (Supplementary Figure S2C and D). Taken together, these data reveal that while many of the properties of Dnmt3b are intrinsic to and maintained in the isolated catalytic domain, the N-terminal domain clearly influences these properties, suggesting that splice variants lacking regions of the N-terminus may possess altered functions *in vivo*.

Influence of ICF syndrome point mutations on Dnmt3b1 protein–DNA interaction, interaction with Dnmt3L, and enzymatic activity

Although a previous study examined the functional consequences of several ICF-associated *Dnmt3b* mutations, the isolated C-terminal domain was used for these experiments (13). Our data show that the N-terminal domain influences several properties previously thought to be linked exclusively to the C-terminus (e.g. Dnmt3L interaction). To examine how these point mutations alter Dnmt3b function in the context of the full-length protein, eight ICF syndrome patient-derived *DNMT3B* mutations were introduced into the homologous positions of murine Dnmt3b1 [Supplementary Table S2, (14)], expressed and purified from baculovirus infected Sf9 cells. EMSA DNA binding analysis using the SAT2 probe, one of the sequences invariantly hypomethylated in ICF syndrome patients (11), revealed that all ICF Dnmt3b mutations mildly to moderately (e.g. R846Q K_D = 303 nM) reduced DNA binding affinity, although all eight mutants clearly retain the ability to bind DNA (Figure 4A and Table 1).

The Dnmt3b–Dnmt3L interaction, assessed using GST pull downs, showed that, with the exception of the G669S mutant, all other ICF Dnmt3b mutations caused a reduction in the strength of the Dnmt3b–Dnmt3L interaction compared to the WT form (Figure 4B and Table 1). For example, the V612A mutation immediately adjacent to conserved motif I interacted only weakly with Dnmt3L in the low ionic strength buffer conditions. Sequences adjacent to conserved motif X (e.g. the R829G mutation) also appear to play an important role in the Dnmt3b–Dnmt3L interaction (Figure 4B and Table 1). Our results are, at least qualitatively, similar to those reported in an earlier study of Dnmt3b–Dnmt3L interactions using a similar panel of mutations in the context of the isolated C-terminal domain of Dnmt3b in a mammalian two-hybrid assay (14), with the exception of the R829Q mutant. The differences may be attributable to our use of the full-length form of Dnmt3b1 for all assays.

When levels of enzymatic activity were examined, the L670T, V732G, A772P and H820R mutations were essentially inactive when tested with the SAT2 and plasmids sequences in pyrosequencing assays. Less than 1% methylation was detected without Dnmt3L and < 2% methylation was detected in the presence of Dnmt3L for the L670T, V732G, A772P mutants. While these values may reflect bona fide residual activity in the presence of Dnmt3L detectable because of the high sensitivity and reproducibility of the pyrosequencing assays, it is still sufficiently low that its biological significance, if any, is questionable (Figure 4C, Supplementary Figure S3A and Table 1). Interestingly this low-level activity is only observed with the SAT2 sequence, not the plasmid. The R829G and R846Q mutants, despite having reduced DNA binding affinity and ability to interact with Dnmt3L, retained a low level of activity alone that was stimulated by Dnmt3L, on a fold-change basis, to levels comparable with wild-type Dnmt3b1 (Table 1). We also used the pyrosequencing data to examine whether ICF syndrome-associated mutations altered CpG preference of Dnmt3b. Analysis of the SAT2 and plasmid regions indicated that all mutations reduced activity proportionally at all CpG sites rather than exerting an effect on a subset of sites (Supplementary Figure S4). BGS analysis also confirmed the pyrosequencing data over the larger SAT2 and plasmid backbone regions, reinforcing the conclusion that ICF syndrome-associated point mutations do not alter the intrinsic CpG site preferences of Dnmt3b (Figure S3B and C). Curiously, the activity of the V612A mutant, which displayed impaired but not abolished ability to interact with Dnmt3L, was actually repressed upon addition of Dnmt3L for the SAT2

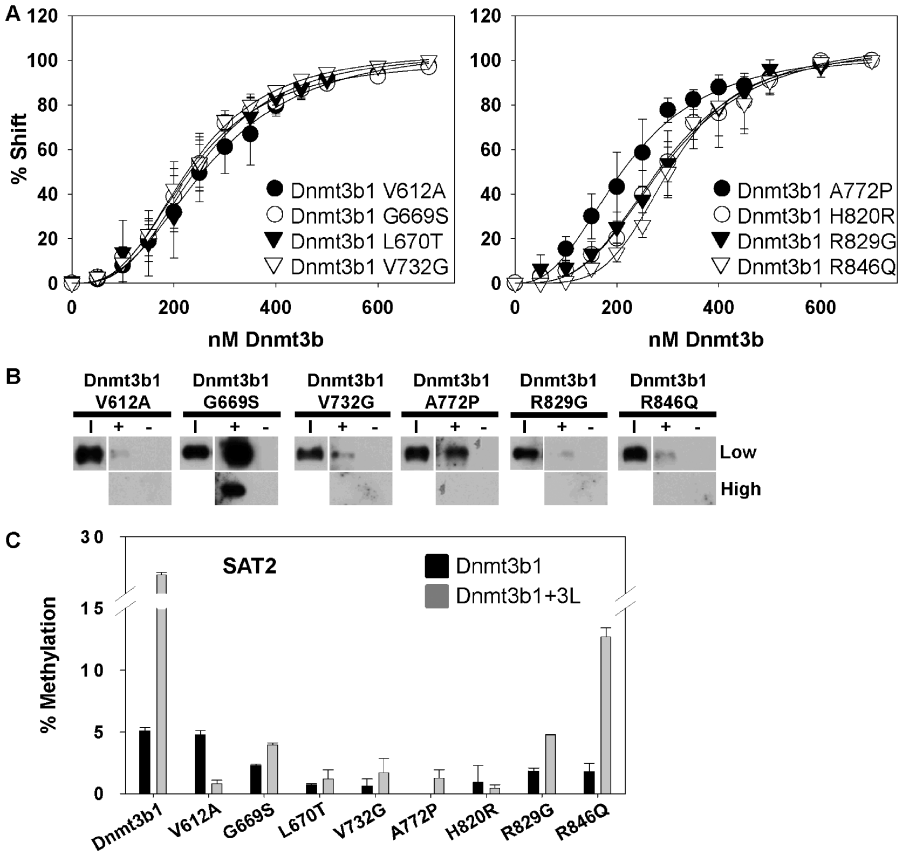

Figure 4. Functional effects of ICF syndrome mutations on Dnmt3b1 protein–DNA interactions, interaction with Dnmt3L, and enzymatic activity. (**A**) Quantification of EMSA gels and Hill plots summarizing the binding of each Dnmt3b1 mutant (0–700 nM) to the SAT2 DNA probe. (**B**) Representative western blots showing protein–protein interactions of Dnmt3b1 mutants and GST-Dnmt3L by GST pull down as described in Figures 2B and 3B. (**C**) Pyrosequencing-based determination of overall percent methylation of the SAT2 sequence by mutant Dnmt3b1 isoforms with and without Dnmt3L.

sequence (Table 1). Our data are largely in agreement with those obtained by Gowher *et al.* (13) who used several of the same mutations we examined in the context of the isolated Dnmt3b catalytic domain even though completely different assays were used to detect methylation. With the exception of the A772P and R846Q mutants, our results are also similar to those reported in a later study (14) using many of the same mutants in the context of full-length Dnmt3b1 expressed in bacteria. Differences may be attributable to the use of different buffer conditions and DNA substrates, or our use of the more sensitive pyrosequencing method to assess DNA methylation levels. In any case, our data clearly support the notion that ICF syndrome-associated *Dnmt3b* mutations have diverse effects on multiple properties of Dnmt3b that likely contribute to patient phenotypic variability.

Consequences of alternative splicing, domain deletions, and ICF syndrome-associated point mutations on Dnmt3b self-interactions

It has become clear from structural studies that not only is the Dnmt3a–Dnmt3L interaction important for Dnmt3a's biological activity, but also the ability of Dnmt3a to interact with itself and mediate formation of the 3L–3a–3a–3L heterotetramer proposed to represent the active form of Dnmt3a in cell types that co-express both proteins (29). We have shown previously limited evidence for a Dnmt3b1–Dnmt3b3 interaction using the yeast two hybrid assay (24), and the DNMT3B7 splice variant was recently shown to interact with other endogenous Dnmt3b isoforms by co-immunoprecipitation (20); however, Dnmt3b–Dnmt3b 'self' interactions have not, to our knowledge, been examined rigorously. To investigate this, we utilized GST pull downs under the same low and moderate stringency conditions used to study the Dnmt3b–Dnmt3L interaction. The C-terminal domains of Dnmt3b1 and Dnmt3b3 were fused to GST and expressed in *E. coli* as the 'bait'. Hexahistidine tagged Dnmt3b constructs, purified from baculovirus infected Sf9 cells (the 'prey'), were incubated with GST fusions and interactions monitored by western blotting with an antibody directed against the 6XHis tag. The Dnmt3b1 C-terminus interacted with full-length Dnmt3b1 and Dnmt3b3 isoforms, but, interestingly, did not interact with Dnmt3b2 (Figure 5A and Table 1). Results from pull downs using the Dnmt3b3 C-terminus were similar except that all interactions were, unexpectedly, more robust than for the Dnmt3b1 C-terminus (e.g. the Dnmt3b3 C-terminus interacted with Dnmt3b2, albeit weakly, under the lower stringency conditions, Figure 5B and Table 1). The Dnmt3b3 C-terminus

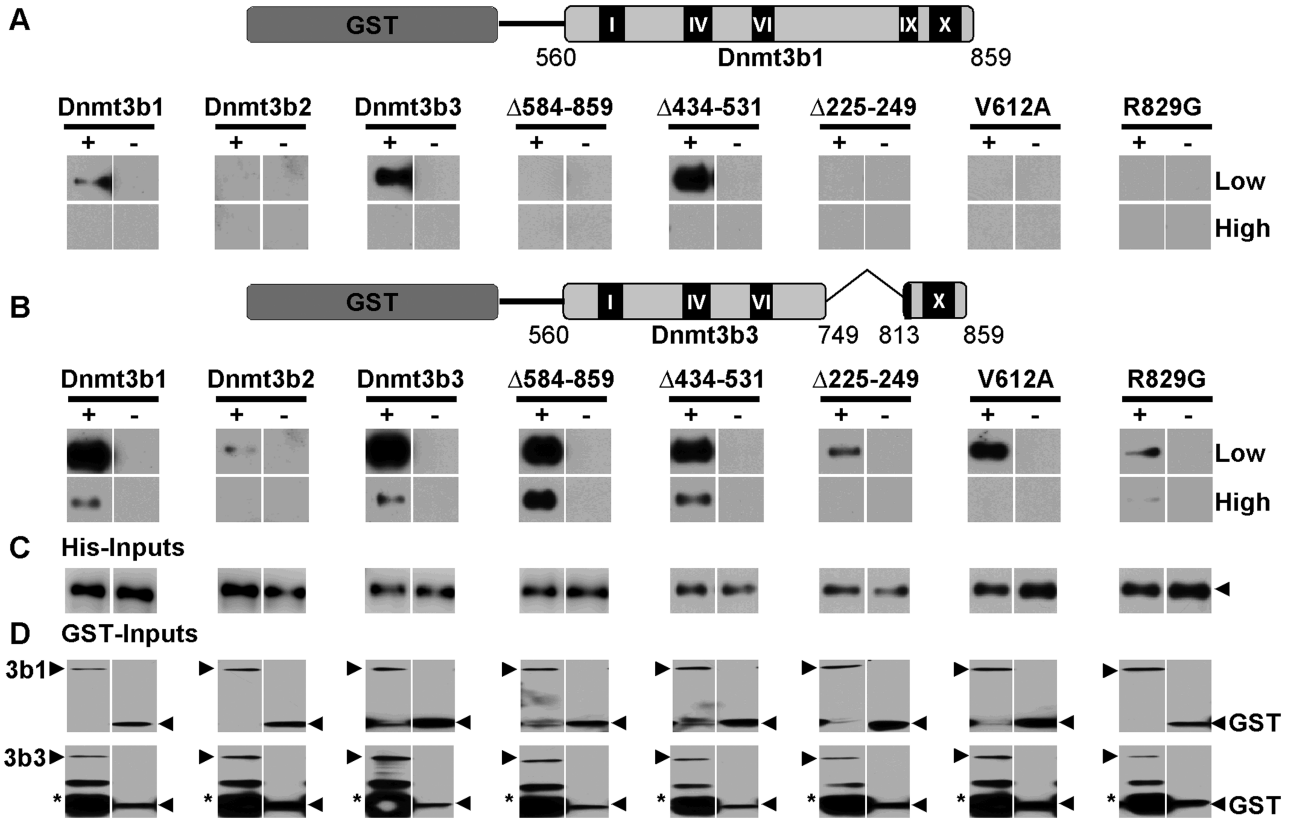

Figure 5. Impact of alternative splicing, domain deletions and ICF syndrome-associated mutations on Dnmt3b1 interaction with the catalytic domains (CD) of Dnmt3b1 and Dnmt3b3. (**A**) Top panel: schematic of the GST-tagged catalytic domain of Dnmt3b1 used for protein–protein interaction pull downs. Catalytic motifs are indicated by roman numerals. Numbering indicates amino acids of Dnmt3b present in the construct. Bottom panel: representative western blots using anti-6XHis tag antibody to study protein–protein interactions between the indicated Dnmt3′s and GST-Dnmt3b1 CD. +, pull down with GST-Dnmt3b1 CD;−,pull down with GST (negative control), low and high refer to the 100 and 150 mM KCl used in binding reaction/washes, respectively. (**B**) Top panel: schematic of the Dnmt3b3 catalytic domain-GST fusion protein used for pull downs. Numbering denotes amino acids of Dnmt3b present in the construct and the alternatively spliced region characteristic of Dnmt3b3. Bottom panel: representative western blots using anti-6XHis tag antibody to detect protein–protein interactions between the indicated Dnmt3 constructs and GST-Dnmt3b3 CD. (**C**) 6X-His fusion protein and (**D**) GST-fusion protein inputs used in the pull down reactions to demonstrate equal loading. Reactions identical to the pull downs (without washing) were run with the pull down reactions and proteins detected by western blotting with antibodies against the 6XHis or GST tags. Arrowhead—specific protein, asterisk—non-specific band.

also interacted robustly with the isolated Dnmt3b1 N-terminal domain. This result is consistent with the observation that DNMT3B7 interacts with other DNMT3B isoforms (20) as well as with earlier studies where the N- and C-terminal domains of DNMT1 were shown to interact (37). Dnmt3a interacted strongly with both the Dnmt3b1 and Dnmt3b3 C-termini (Table 1). It is also possible that the interactions we observe are, to some extent, modulated by which partner is free in solution (6XHis-tagged) versus bound to a solid support (GST-tagged). Such effects might, for example, explain differences in binding affinity between Dnmt3b1 and Dnmt3b3 (compare Figure 5A third panel to Figure 5B first panel). Differences in binding between the Dnmt3b1-CD and the Dnmt3b3-CD are not attributable to variability in the amounts of input proteins as these are comparable across all pull downs (Figure 5C and D).

Our GST pull down experiments using the Dnmt3b domain deletions revealed that interactions involving the C-terminus of the Dnmt3b1 isoform were much more sensitive to deletions within the C-terminal domain, as would be predicted from the Dnmt3a structure [(29) and Figure 1]. Deletions within the Dnmt3b1 N-terminus [e.g. amino acids 1–140 and the PWWP domain], however, also weakened or abolished interactions with the Dnmt3b1 C-terminus (Figure 5A and Table 1). In contrast, the Dnmt3b3 C-terminus interacted moderately to strongly with all domain deletions (Figure 5B and Table 1). Interestingly, the active site point mutant, Dnmt3b1 C657A, completely lost the ability to interact with both the Dnmt3b1 and Dnmt3b3 C-terminal GST fusion constructs (this same mutation had no effect on the Dnmt3b–Dnmt3L interaction). With the exception of the ICF syndrome-associated V612A and R829G mutations, all Dnmt3b1 point mutants interacted with both the Dnmt3b1 and Dnmt3b3 C-terminal GST fusions, suggesting that the majority of ICF mutations do not disrupt this interaction (Figure 5 and Table 1). Taken together, these results demonstrate that Dnmt3b makes extensive interactions with itself and with other alternatively spliced Dnmt3b isoforms and that most ICF syndrome-associated *Dnmt3b* mutations do not impair

self-interaction (i.e. the ability of WT Dnmt3b to interact with ICF mutant Dnmt3b). Regions of both the N- and C-terminus of Dnmt3b are important for self-interaction, including the catalytic center. Surprisingly, Dnmt3b3, which lacks a portion of the catalytic domain and might, based on the Dnmt3a crystal structure data (29), be predicted not to self-interact, actually interacted more robustly and promiscuously with all other Dnmt3b isoforms and mutants, suggesting that this widely expressed but catalytically inactive isoform binds to and perhaps modulates the activity of catalytically competent Dnmt3a and Dnmt3b proteins *in vivo* in cells where they are co-expressed.

Trimolecular Dnmt3 interactions: effects of Dnmt3b isoforms and mutants on the activity of Dnmt3a–Dnmt3L

Given our previous data that Dnmt3b forms extensive interactions with other Dnmt3b isoforms, Dnmt3a and Dnmt3L, and others' data that Dnmt3b in ES cells exists in a complex with Dnmt3a and Dnmt3L (2,3), we next asked how addition of all three Dnmt3s to the same reaction would affect methylation activity. Although all three proteins co-purify, the exact composition and stoichiometry of this complex is unknown [e.g. a 3L–3a–3b–3L complex or some other higher order complex interaction as suggested by recent scanning force microscopy experiments (38)]. Therefore Dnmt3a, Dnmt3b1 and Dnmt3L, in an equimolar ratio, were co-incubated with the SAT2-containing plasmid and SAM for 7 h. Digestion of *in vitro* methylated DNA with HpaII followed by gel quantitation revealed that a Dnmt3a–Dnmt3b1–Dnmt3L-containing reaction had higher activity than either Dnmt3a–Dnmt3L or Dnmt3b1–Dnmt3L bimolecular reaction, however the total activity was essentially additive (that is a sum of the Dnmt3b1+Dnmt3L and Dnmt3a+Dnmt3L activities) rather than synergistic. Similar results were obtained using pyrosequencing to assess methylation levels at the SAT2 and plasmid regions (Figure 6, Supplementary Figure S5 and Table 1). Activity of a trimolecular reaction containing Dnmt3b2 also yielded activity approximately equivalent to individual Dnmt3b2+Dnmt3L and Dnmt3a+Dnmt3L reactions. Addition of proteins in different sequences with preincubation (e.g. Dnmt3b+Dnmt3L then add Dnmt3a) did not change activity levels (data not shown).

Of particular interest, however, was the finding that mixing catalytically inactive Dnmt3b isoforms (e.g. Dnmt3b1 C657A, Dnmt3b3 or inactive ICF mutants) 'stimulated' the activity of Dnmt3a and Dnmt3L in the reaction mixtures as much as catalytically competent Dnmt3b isoforms (by ~20–30%, Figure 6, Supplementary Figure S5 and Table 1). This effect is clearly a stimulation of Dnmt3a–Dnmt3L activity because our prior experiments showed that these Dnmt3b isoforms/mutants had no enzymatic activity in the absence or presence of Dnmt3L in multiple independent assays. Additional experiments mixing other inactive Dnmt3b isoforms (e.g. C657A) with Dnmt3b3, in the absence of Dnmt3L, also showed no evidence for Dnmt3b3 having enzymatic activity (data not shown). Activity of Dnmt3a–Dnmt3L on the plasmid was

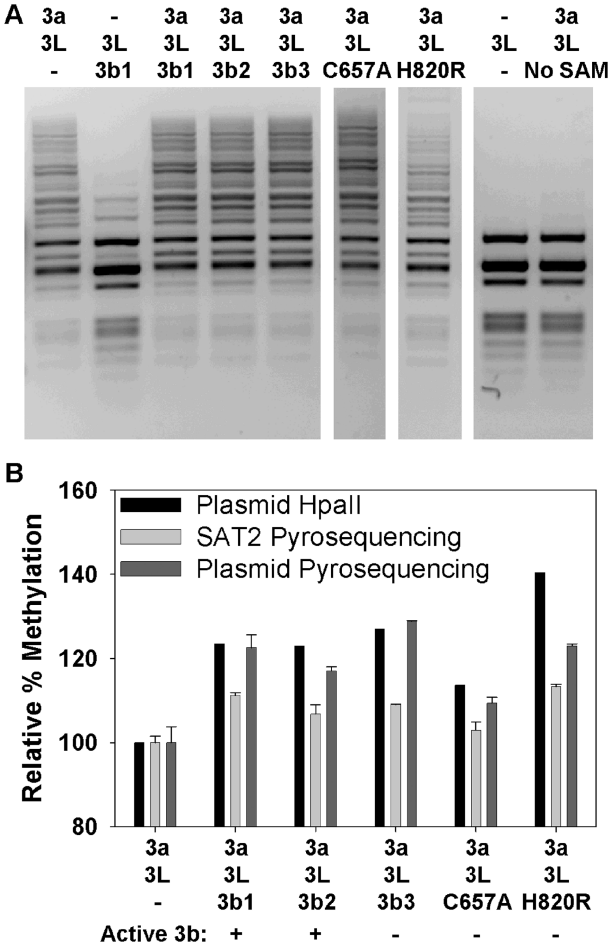

Figure 6. Effects of Dnmt3b alternative splicing, deletions and ICF syndrome-associated mutations on the enzymatic activity of Dnmt3a combined with Dnmt3L. (**A**) Representative HpaII restriction digests of SAT2-containing plasmid following methyltransferase activity assay combining Dnmt3a and Dnmt3L with the indicated Dnmt3b proteins. Lanes 8 (no Dnmt3) and 9 (no SAM) are negative controls. (**B**) Effects of select Dnmt3b constructs on methylation of the SAT2 sequence when mixed with Dnmt3a+Dnmt3L relative to Dnmt3a+Dnmt3L alone. Percent methylation is quantitated by HpaII digestion (black bars) and pyrosequencing at both the SAT2 and plasmid regions (light and dark gray bars, respectively), relative to a reaction with only Dnmt3a+Dnmt3L. Active 3b: +, construct has demonstrated activity alone; –, construct does not possess catalytic activity alone.

generally stimulated to a greater extent by Dnmt3b than the Dnmt3a–Dnmt3L activity toward SAT2 (assessed by pyrosequencing). The stimulation of Dnmt3a–Dnmt3L by inactive Dnmt3b isoforms, while modest, was highly reproducible. Dnmt3b isoforms generally increased methylation at all CpG sites rather than targeting a few specific sites for increase (Supplementary Figure S5). All ICF syndrome-associated Dnmt3b point mutants, regardless of their activity in isolation or in combination with Dnmt3L, stimulated Dnmt3a–Dnmt3L activity (Figure 6, Supplementary Figure S5 and Table 1). Deletion of the PWWP domain (amino acids 225–249) reduced Dnmt3b1 stimulation and deletion of amino acids 227–429 reduced it further, suggesting an important role for residues 250–429 in mediating this effect. Deletion of

the extreme C-terminus (amino acids 671–859) of Dnmt3b1 also abolished the stimulatory effect on Dnmt3a–Dnmt3L (Supplementary Figures S5B and E, Table 1). The ability of some Dnmt3b1 deletions/splice variants, but not others, to stimulate Dnmt3a–Dnmt3L activity argues against this effect being due to non-specific protein–protein interactions or buffer effects. Deletion of these same regions also impairs Dnmt3b1 self-interactions (Table 1). Although at present we do not know the exact composition of the complexes or interactions that occur in the Dnmt3b–Dnmt3a–Dnmt3L-containing reactions, our data suggest that Dnmt3b is capable of modulating the activity of Dnmt3a–Dnmt3L complexes independent of its catalytic activity via residues within both the N- and C-terminal domains. Our data are consistent with an *in vivo* study showing that a catalytically inactive Dnmt3a point mutant stimulated Dnmt3b methylation of the *Oct4* promoter in ES cells, which also express high levels of Dnmt3b (3).

In vivo versus *in vitro* SAT2 DNA methylation patterns and Dnmt3b/Dnmt3L cellular localization

Our data thus far is derived entirely from *in vitro* studies and as such lacks the information provided to Dnmt3b by chromatin structure and the histone code. To begin to extend the relevance our findings to the *in vivo* regulation of DNA methylation, we compared patterns of SAT2 methylation derived from the *in vitro* studies here, with our previous analysis of SAT2 DNA methylation patterns in the HCT116 colorectal cancer cell line generated by traditional BGS (18,24). This analysis revealed that CpG sites preferred by Dnmt3b *in vitro* are also preferred sites of methylation *in vivo* (Supplementary Figure S6). *In vitro* Dnmt3a SAT2 methylation patterns, in contrast, showed no correlation with SAT2 methylation patterns in HCT116 cells.

We next examined the cellular localization of Dnmt3b1, Dnmt3b2 and Dnmt3b3 alone and with Dnmt3L by fusing the open reading frame of each to green or red fluorescent proteins (GFP/RFP), transfecting the plasmids into human HEK293T cells, and visualizing each Dnmt using confocal microscopy. Dnmt3b1 and Dnmt3b3 displayed exclusively nuclear staining with enrichment in 'DAPI'-dense regions of heterochromatin (Dnmt3b1 enrichment in these regions was greater than Dnmt3b3, representative images are shown in Figure 7A). While the nuclear staining of Dnmt3b2 was similar to that of Dnmt3b1/3b3, almost 50% of cells displayed some cytoplasmic staining (Figure 7A, compare two cells in Dnmt3b2 panel). Dnmt3L was equally distributed throughout the nucleus and cytoplasm. The majority of each Dnmt3b colocalized with nuclear Dnmt3L upon co-transfection. Fewer cells displayed cytoplasmic localization of Dnmt3b2 and Dnmt3L was more concentrated in the nucleus in co-transfected cells (Figure 7B). Similar results were obtained when Dnmt3b2 and Dnmt3b3 were co-transfected with Dnmt3b1 (Figure 7C). We also examined localization of the Dnmt3b1 C657A mutant (showing normal Dnmt3L but abolished Dnmt3b1/3b3 interaction *in vitro*), the Dnmt3b1 Δ227–429, and the Dnmt3b1 V612A ICF mutants (both displayed weakened Dnmt3L/Dnmt3b interaction *in vitro*, Table 1) alone and with Dnmt3b1. 293T cells singly transfected with Dnmt3b1 C657A or Dnmt3b1 V612A displayed localization patterns very similar to WT Dnmt3b1 (although the Dnmt3b1 C657A foci were larger), while the Dnmt3b1 Δ227–429 mutant was distinct; localizing predominantly to the cytoplasm (diffuse and focal concentrations, Figure 7D). These patterns changed little when Dnmt3b1 C657A or Dnmt3b1 V612A were co-transfected with Dnmt3b1, but a fraction of the Dnmt3b1 Δ227–429 mutant became nuclear when co-transfected with Dnmt3b1 (Figure 7E), supporting our *in vitro* data that while the Dnmt3b1 Δ227–429—Dnmt3b1 interaction is weakened (Table 1), they are still capable of interacting. Taken together, these results show that some isoforms/mutants of Dnmt3b displaying altered properties *in vitro* also show distinctive localization patterns *in vivo*. These data also illustrate that other factors are likely influencing Dnmt3b localization *in vivo*, such as chromatin and the presence of endogenous wild-type Dnmt3b and Dnmt3a. As such, while *in vitro* studies are capable of revealing novel functional properties of Dnmt3b because they allow for rigorous control over its environment, future *in vivo* studies will also be essential for fully understanding how specific domains and protein–protein interactions regulate Dnmt3b's function.

DISCUSSION

In the present study, we examined the consequences of alternative splicing, deletion of specific domains and disease-associated point mutations on the ability of Dnmt3b to bind a native target DNA sequence (SAT2), to interact with itself, Dnmt3a and Dnmt3L, and to methylate several different DNA substrates using a comprehensive panel of *in vitro* assays. Our data reveal several important and novel findings. First, naturally occurring (Dnmt3b2) and ubiquitously expressed (Dnmt3b3) splice variants resulted in Dnmt3b proteins with reduced DNA binding affinity and altered ability to interact with itself and Dnmt3L. These isoforms had little effect on Dnmt3b's interaction with Dnmt3a and did not alter CpG site preferences (for Dnmt3b2). Second, all ICF syndrome-associated Dnmt3b mutants, in the context of the full-length protein, resulted in decreased DNA binding affinity and all, except the G669S mutant, displayed decreased binding affinity for Dnmt3L. The Dnmt3b L670T, V732G, A772P and H820R mutants were catalytically inactive. Dnmt3b R829G and R846Q mutants retained activity, which was enhanced by Dnmt3L, even though these mutations reduced both DNA binding affinity and Dnmt3L interaction. Similar to our findings using the domain deletions and splice variants, none of the ICF syndrome Dnmt3b mutations altered CpG site preference or impaired Dnmt3b self-interactions. Third, while the Dnmt3b3 isoform was catalytically inactive; unexpectedly, it was able to interact with all other Dnmt3b isoforms, domain deletions, ICF syndrome mutants and Dnmt3a as well as, and in most cases better, than the

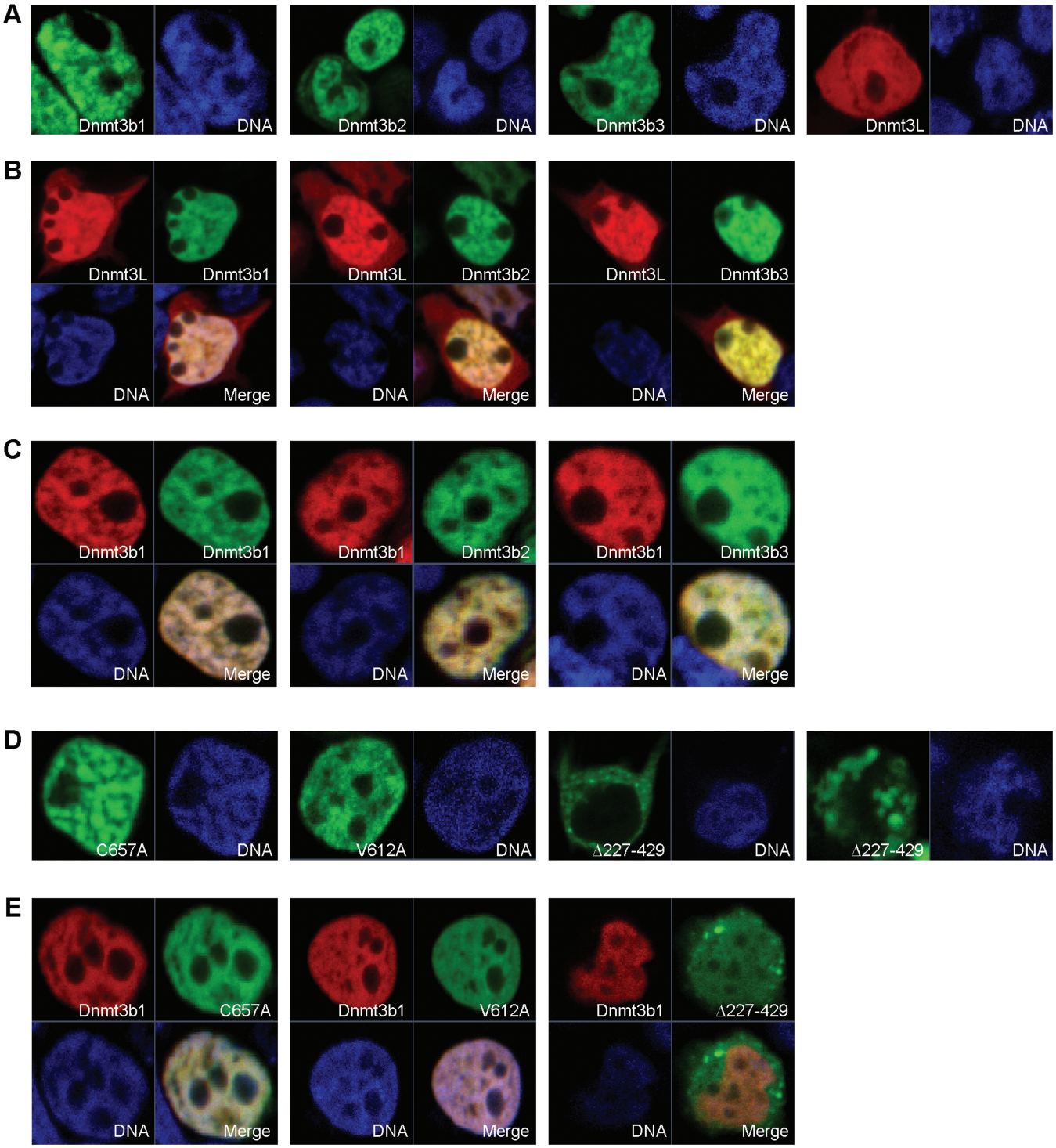

Figure 7. Localization of Dnmt3b isoforms/mutations and Dnmt3L in transiently transfected HEK 293T cells. (**A**) Representative cells showing localization of indicated GFP-tagged Dnmt3b splice variants and DsRed-tagged Dnmt3L when transfected alone. (**B**) Representative cells showing colocalization of GFP-tagged Dnmt3b splice variants with DsRed-tagged Dnmt3L when cotransfected. (**C**) Representative cells showing colocalization of GFP-tagged Dnmt3b splice variants with DsRed-tagged Dnmt3b1when cotransfected. (**D**) Localization of GFP-tagged Dnmt3b1 C657A catalytic mutant, Dnmt3b1 V612A ICF syndrome mutant, and the Dnmt3b1 Δ227–429 deletion construct when transfected alone. Two patterns representative of the population of transfected cells are shown for the Δ227–429 construct. (**E**) Representative cells showing colocalization of GFP-tagged Dnmt3b1 C657A catalytic mutant, Dnmt3b1 V612A ICF syndrome mutant, and Dnmt3b1 Δ227–429 co-transfected with DsRed-tagged Dnmt3b1.

full-length Dnmt3b1 isoform. Fourth, catalytically inactive Dnmt3b isoforms or mutants stimulated Dnmt3a–Dnmt3L complex activity and active Dnmt3b isoforms did not synergize with Dnmt3a–Dnmt3L under our *in vitro* conditions. Fifth, although DNA binding, activity and interaction with Dnmt3L have been previously linked to the C-terminal catalytic domain of Dnmt3b, our studies using full-length isoforms clearly show that the isolated C-terminal domain is impaired in most of these functions relative to full-length protein and that the N-terminal domain makes important contributions to these properties. Finally, microscopic examination of cells transfected with fluorescent Dnmt3 constructs support the *in vitro* data that splicing/mutations impact on *in vivo* functions, but also show that other factors, such as chromatin structure, likely play a role. Taken together, these data reveal novel modulatory functions for the N-terminal domain of Dnmt3b and that catalytically inactive isoforms of Dnmt3b are able to modulate the activity of Dnmt3a–Dnmt3L complexes by an as yet unknown mechanism.

An interesting question that arises out of this work, and the work of others (15,16,18,21), is why most cell types possess the capacity to express so many Dnmt3b splice variants. Furthermore, why are many of these co-expressed in the same cell? There is clear evidence that some alternatively spliced isoforms of Dnmt3b possess altered functions. For example, the widely expressed Dnmt3b3 isoform is catalytically inactive (Table 1). Other consequences of alternative splicing include altered ability to interact with other proteins. Our work here clearly shows that these latter two possibilities do in fact occur with the Dnmt3b2 and Dnmt3b3 splice variants. Furthermore, *in vivo*, alternatively spliced Dnmt3b isoforms may be targeted to different regions of chromatin based on altered protein–protein interactions or changes in the pattern of histone marks that Dnmt3b is recruited to or repelled from by exclusion of specific regions, such as the PWWP domain that was recently reported to bind H3K36 trimethylation [in the context of Dnmt3a (39)]. Alternatively, Dnmt3b splice variants, particularly those lacking catalytic activity, may function as rheostats to fine tune Dnmt3b activity by altering its ability to interact with Dnmt3a and/or Dnmt3L, with other interaction partner(s), or with particular chromatin signatures *in vivo*. They may also change the properties of Dnmt3a when complexed together. Catalytically inactive DNMT3B4 and DNMT3B3Δ5, when overexpressed, result in genomic hypomethylation, suggesting they inhibit or compete for binding to the same DNA sequences as other active Dnmt3 isoforms (18,19). Inactive Dnmt3b isoforms may stimulate active Dnmt3a/Dnmt3b (with or without Dnmt3L)-containing complexes. This notion is supported by our *in vitro* data and results of others showing that overexpression of the DNMT3B7 splice variant results in both hypo- and hypermethylation events *in vivo* (15,20) and that an inactive form of Dnmt3a stimulated Dnmt3b methylation of the *Oct4* promoter *in vivo* (3). Dnmt3b splice variants could also titrate Dnmt3a/Dnmt3L away from active isoforms of Dnmt3b1; however, this may not necessarily be to reduce activity as we have shown that inactive Dnmt3b variants have the capacity, albeit limited, to stimulate the activity of Dnmt3a/Dnmt3L complexes. Alternate splicing may, therefore, represent one of the major mechanisms for regulating overall Dnmt3b activity. Continued transcription of the *Dnmt3b* gene with highly regulated alternative splicing, rather than silencing of the locus, may permit rapid changes in Dnmt3b activity, allowing it to respond more quickly to stimuli.

The impact of Dnmt3L on Dnmt3a has been more extensively studied compared to Dnmt3b both *in vitro* and *in vivo*. Dnmt3b is, in general, expressed earlier than Dnmt3a during embryonic development and both are expressed in a tissue-specific manner (5,40). Dnmt3L expression coincides with Dnmt3a expression during development of the testis while it coincides with Dnmt3b expression in the ovary after birth (41). Interestingly, germ cell-specific knockouts of *Dnmt3a* and *Dnmt3L* yielded remarkably similar phenotypes—both largely affecting methylation patterns at imprinted regions. In contrast, pericentromeric repeats, established targets of Dnmt3b, were not affected in any of the *Dnmt3L* knockout mice (42–44). The nature and importance of Dnmt3b–Dnmt3L interactions during development therefore remains uncertain. Our studies shed some new light on the Dnmt3b–Dnmt3L interaction. Dnmt3L increased the activity of all active Dnmt3b isoforms, deletions, and three of the ICF syndrome mutants. Dnmt3L did not alter Dnmt3b CpG sequence preference, but did enhance its processivity. Dnmt3L also enhances the processivity of Dnmt3a based on a recent study (34) suggesting that this is a conserved function of Dnmt3L. Notably, CpGs that had the lowest levels of methylation by Dnmt3b in the absence of Dnmt3L, displayed the greatest increase in methylation upon Dnmt3L addition. An identical effect of Dnmt3L on Dnmt3a was also recently reported (45). All of our Dnmt3b constructs, with the exception of the Δ671–859 mutant, interacted with Dnmt3L at the lower salt concentration. Loss of Dnmt3b–Dnmt3L interaction at the higher salt condition, interestingly, did not predict loss of Dnmt3L stimulation of Dnmt3b in activity assays, suggesting that a strong or extended interaction is unnecessary for Dnmt3L to exert its effects. Another novel observation from our work is that Dnmt3L enhanced the DNA binding affinity of DNMT3B1 on the SAT2 probe. A prior study reported that Dnmt3L did not bind DNA on its own (46), consistent with our findings. This same study also showed that Dnmt3L increased Dnmt3b mobility in a gel shift assay suggesting that Dnmt3L dissociates Dnmt3b1 aggregates, exposing the catalytic domain to the DNA and enhancing activity (46). Dnmt3L may alter the conformation of the DNA binding region of Dnmt3b in a way that enhances its affinity for DNA. In addition, our data show that the N-terminal domain of Dnmt3b, while not essential, does influence Dnmt3b's ability to bind Dnmt3L in the context of the full-length protein. Dnmt3b sequences, including and in particular C-terminally flanking the PWWP domain, were also important for Dnmt3b–Dnmt3b interactions. The PWWP domain of Dnmt3a contains an allosteric DNA binding site that alters Dnmt3a catalytic activity and self-interaction (aggregation) (47),

supporting our findings that the PWWP domain and flanking sequences are important for several of Dnmt3b's properties.

An unexpected finding based on our *in vitro* pull down experiments was that the Dnmt3b3 isoform interacted more strongly and more promiscuously with almost all other Dnmt3b isoforms/deletions/mutations and Dnmt3a. Only the interaction between Dnmt3b3 and Dnmt3L appeared somewhat weaker than the Dnmt3b1–Dnmt3L interaction. Most of the ICF syndrome *Dnmt3b* mutants also followed this trend, except for the L670T mutation (present in the Dnmt3b–Dnmt3L interface/active site loop region based on the Dnmt3a–Dnmt3L structure) and the A772P mutation (proposed to influence Dnmt3a stability) (29), which interacted with the Dnmt3b1 and Dnmt3b3 C-termini equally well (Table 1). This study postulated that the H814R, D817G and V818M DNMT3B ICF syndrome mutation were located in the Dnmt3b–Dnmt3b interface and would be unable to self-interact (29). Although, we have not examined all possible ICF syndrome mutations here, mutation of nearby residues (H820R and R829G) clearly impacted Dnmt3b self-interactions involving Dnmt3b1 but had far less impact on interactions involving Dnmt3b3. Ueda *et al*. (48) also analyzed some of the same mutations and reported that the L670T, V732G, A772P and D823G Dnmt3b mutations did not disrupt Dnmt3a–Dnmt3b interaction using co-immunoprecipitation assays, but the A609T ICF mutation did abolish interaction. The V612A and R829G mutations we analyzed were unable to interact with Dnmt3b1 based on our pull down assays. The Dnmt3a–Dnmt3L structural studies (29) collectively suggested that exclusion of exons 22 and 23 (in murine Dnmt3b3) would eliminate Dnmt3b self-interactions. Our data do not support this notion, suggesting that Dnmt3b interacts with itself differently than Dnmt3a and/or that the Dnmt3b N-terminus (which also mediates self-interaction) is compensating for mutations in the C-terminal domain. Interestingly, an alternatively spliced isoform of Dnmt3a resembling Dnmt3b3 has not, to our knowledge, been identified suggesting that there may be important differences in the way Dnmt3a and Dnmt3b interact with themselves, and possibly also with Dnmt3L. The lack of C-terminal exons 22 and 23 might cause Dnmt3b3 to adopt a more open structure compared to the catalytically active Dnmt3b1 isoform, permitting greater flexibility in what it interacts with.

We believe that our findings, based on *in vitro* data, have potential relevance to the DNA methylation changes that occur in transformed cells. Tumor cells exhibit both hypo- and hypermethylation defects (7). While a mechanism such as elevated DNMT expression could explain the hypermethylation events, it does little to account for genomic hypomethylation. Improper expression of normal Dnmt3b splice variants [such as DNMT3B4 (19)] in the wrong cell type or *de novo* expression of aberrant transcripts during tumorigenesis [such as DNMT3B7 (20)] represents an attractive alternative mechanism able to account for both types of methylation defects that occur in cancer cells. Our data, and that of others (20), show that full-length Dnmt3b isoforms interact with other mutant forms of Dnmt3b that contain only the N-terminal regulatory domain. Our Dnmt3b1 Δ584–859 mutant interacts with the full-length Dnmt3b3 isoform and DNMT3B7 (containing the first 360 amino acids of DNMT3B1) co-immunoprecipitates with other DNMT3B isoforms (20). Interestingly, both of these isoforms lack the Dnmt3b–Dnmt3b interface predicted from structural studies (29). Furthermore, our EMSA data revealed the presence of a strong DNA binding domain in the context of the first 433 amino acids of Dnmt3b1. These findings may have relevance in tumor cells that express C-terminally truncated forms of Dnmt3b because they suggest that the truncated form interacts with other 'normal' Dnmt3b isoforms. Such an interaction could alter the activity, DNA binding, or Dnmt3a/Dnmt3L interaction of normal Dnmt3b isoforms. In addition, because of the strong affinity for DNA of N-terminal Dnmt3b fragments, they may out-compete normal Dnmt3b isoforms with their lower DNA binding affinity or recruit active Dnmt3b isoforms to sequences not normally targeted by Dnmt3b. Any of these scenarios could result in loss of Dnmt3b-mediated DNA methylation at normal targets and promote *de novo* methylation at abnormal targets *in vivo*. As such, further characterization of the functional consequences of Dnmt3b alternative splicing may provide important insights into the molecular underpinnings of tumor-associated global DNA methylation defects.

SUPPLEMENTARY DATA

Supplementary Data are available at NAR Online.

ACKNOWLEDGEMENTS

We thank Guo-Liang Xu and Taiping Chen for supplying plasmids and Hongyan Xu for assistance with statistical analysis.

FUNDING

National Institute of Health grants R01CA116028, R01CA114229 (K.D.R.), F32CA132327 (B.O.V.) and the Georgia Cancer Coalition (K.D.R.). K.D.R. is a Georgia Cancer Coalition Distinguished Cancer Scholar. Funding for open access charge: Georgia Health Sciences University startup funds.

Conflict of interest statement. None declared.

REFERENCES

1. Kareta,M.S., Botello,Z.M., Ennis,J.J., Chou,C. and Chedin,F. (2006) Reconstitution and mechanism of the stimulation of *de novo* methylation by human DNMT3L. *J. Biol. Chem.*, **281**, 25893–25902.
2. Ooi,S.K.T., Qiu,C., Bernstein,E., Li,K., Jia,D., Yang,Z., Erdjument-Bromage,H., Tempst,P., Lin,S.-P., Allis,C.D. *et al.* (2007) DNMT3L connects unmethylated lysine 4 of histone H3 to *de novo* methylation of DNA. *Nature*, **448**, 714–717.
3. Li,J.-Y., Pu,M.-T., Hirasawa,R., Li,B.-Z., Huang,Y.-N., Zeng,R., Jing,N.-H., Chen,T., Li,E., Sasaki,H. *et al.* (2007) Synergistic

function of DNA methyltransferases Dnmt3a and Dnmt3b in the methylation of *Oct4* and *Nanog*. *Mol. Cell. Biol.*, **27**, 8748–8759.
4. Ooi,S.K.T., O'Donnell,A.H. and Bestor,T.H. (2009) Mammalian cytosine methylation at a glance. *J. Cell. Sci.*, **122**, 2787–2791.
5. Okano,M., Bell,D.W., Haber,D.A. and Li,E. (1999) DNA methyltransferases *Dnmt3a* and *Dnmt3b* are essential for de novo methylation and mammalian development. *Cell*, **99**, 247–257.
6. Gopalakrishnan,S., VanEmburgh,B.O. and Robertson,K.D. (2008) DNA methylation in development and human disease. *Mutat. Res.*, **647**, 30–38.
7. Sharma,S., Kelly,T.K. and Jones,P.A. (2010) Epigenetics in cancer. *Carcinogenesis*, **31**, 27–36.
8. Linhart,H.G., Lin,H., Yamada,Y., Steine,E.J., Gokhale,S., Lo,G., Cantu,E., Ehrich,M., He,T., Meissner,A. *et al.* (2007) Dnmt3b promotes tumorigenesis in vivo by gene-specific de novo methylation and transcriptional silencing. *Genes. Dev.*, **21**, 3110–3122.
9. Hansen,R.S., Stoger,R., Wijmenga,C., Stanek,A.M., Canfield,T.K., Luo,P., Matarazzo,M.R., D'Esposito,M., Feil,R., Gimelli,G. *et al.* (2000) Escape from gene silencing in ICF syndrome: evidence for advanced replication time as a major determinant. *Hum. Mol. Genet.*, **9**, 2575–2587.
10. Jiang,Y.L., Rigolet,M., Bourc'his,D., Nigon,F., Bokesoy,I., Fryns,J.P., Hulten,M., Jonveaux,P., Maraschio,P., Megarbane,A. *et al.* (2005) DNMT3B mutations and DNA methylation defect define two types of ICF syndrome. *Hum. Mut.*, **25**, 56–63.
11. Ehrlich,M., Jackson,K. and Weemaes,C. (2006) Immunodeficiency, centromeric region instability, facial anomalies syndrome (ICF). *Orphanet J. Rare Dis.*, **1**, 2.
12. Jin,B., Tao,Q., Peng,J., Soo,H.M., Wu,W., Ying,J., Fields,C.R., Delmas,A.L., Liu,X., Qiu,J. *et al.* (2008) DNA methyltransferase 3B (DNMT3B) mutations in ICF syndrome lead to altered epigenetic modifications and aberrant expression of genes regulating development, neurogenesis and immune function. *Hum. Mol. Genet.*, **17**, 690–709.
13. Gowher,H. and Jeltsch,A. (2002) Molecular enzymology of the catalytic domains of the Dnmt3a and Dnmt3b DNA methyltransferases. *J. Biol. Chem.*, **277**, 20409–20414.
14. Xie,Z.-H., Huang,Y.-N., Chen,Z.-X., Riggs,A.D., Ding,J.-P., Gowher,H., Jeltsch,A., Sasaki,H., Hata,K. and Xu,G.-L. (2006) Mutations in DNA methyltransferase DNMT3B in ICF syndrome affect its regulation by DNMT3L. *Hum. Mol. Genet.*, **15**, 1375–1385.
15. Ostler,K.R., Davis,E.M., Payne,S.L., Gosalia,B.B., Exposito-Cespedes,J., LeBeau,M.M. and Godley,L.A. (2007) Cancer cells express aberrant *DNMT3B* transcripts encoding truncated proteins. *Oncogene*, **26**, 5553–5563.
16. Weisenberger,D.J., Velicescu,M., Cheng,J.C., Gonzales,F.A., Liang,G. and Jones,P.A. (2004) Role of the DNA methyltransferase variant DNMT3b3 in DNA methylation. *Mol. Cancer Res.*, **2**, 62–72.
17. Robertson,K.D., Uzvolgyi,E., Liang,G., Talmadge,C., Sumegi,J., Gonzales,F.A. and Jones,P.A. (1999) The human DNA methyltransferases (DNMTs) 1, 3a, and 3b: Coordinate mRNA expression in normal tissues and overexpression in tumors. *Nucleic Acids Res.*, **27**, 2291–2298.
18. Gopalakrishnan,S., VanEmburgh,B.O., Fields,C.R., Su,Z., Terada,N. and Robertson,K.D. (2009) A novel DNMT3B splice variant expressed in pluripotent cells and brain with altered DNA binding and nuclear localization. *Mol. Cancer Res.*, **7**, 1622–1634.
19. Saito,Y., Kanai,Y., Sakamoto,M., Saito,H., Ishii,H. and Hirohashi,S. (2002) Overexpression of a splice variant of DNA methyltransferase 3b, DNMT3b4, associated with DNA hypomethylation on pericentromeric satellite regions during human hepatocarcinogenesis. *Proc. Natl Acad. Sci. USA*, **99**, 10060–10065.
20. Shah,M.Y., Vasanthakumar,A., Barnes,N.Y., Figeroa,M.E., Kamp,A., Hendrick,C., Ostler,K.R., Davis,E.M., Lin,S., Anastasi,J. *et al.* (2010) DNMT3B7, a truncated DNMT3B isoform expressed in human tumors, disrupts embryonic development and accelerates lymphomagenesis. *Cancer Res.*, **70**, 5840–5850.
21. Wang,L., Wang,J., Sun,S., Rodriguez,M., Yue,P., Jang,S.J. and Mao,L. (2006) A novel DNMT3B subfamily, DDNMT3B, is the predominant form of DNMT3B in non-small cell lung cancer. *Int. J. Oncol.*, **29**, 201–207.
22. Margot,J.B., Ehrenhofer-Murray,A.E. and Leonhardt,H. (2003) Interactions within the mammalian DNA methyltransferase family. *BMC Mol. Bio.*, **4**, 7.
23. Chen,Z.-X., Mann,J.R., Hsieh,C.-L., Riggs,A.D. and Chedin,F. (2005) Physical and functional interactions between the human DNMT3L protein and members of the de novo methyltransferase family. *J. Cell. Biochem.*, **95**, 902–917.
24. Gopalakrishnan,S., Sullivan,B.A., Trazzi,S., Valle,G.D. and Robertson,K.D. (2009) DNMT3B interacts with constitutive centromere protein CENP-C to modulate DNA methylation and the histone code at centromeric regions. *Hum. Mol. Genet.*, **18**, 3178–3193.
25. Takeshima,H., Suetake,I., Shimahara,H., Ura,K., Tate,S.-i. and Tajima,S. (2006) Distinct DNA methylation activity of Dnmt3a and Dnmt3b towards naked and nucleosomal DNA. *J. Biochem.*, **139**, 503–515.
26. Kumaki,Y., Oda,M. and Okano,M. (2008) QUMA: quantification tool for methylation analysis. *Nucleic Acids Res.*, **36**, W170–175.
27. Lee,B.H., Yegnasubramanian,S., Lin,X. and Nelson,W.G. (2005) Procainamide is a specific inhibitor of DNA methyltransferase 1. *J. Biol. Chem.*, **280**, 40749–40756.
28. Qiu,J., Ai,L., Ramachandran,C., Yao,B., Gopalakrishnan,S., Fields,C.R., Delmas,A.L., Dyer,L.M., Melnick,S.J., Yachnis,A.T. *et al.* (2008) Invasion suppressor CST6 (cystatin E/M): High-level cell type-specific expression in normal brain and epigenetic silencing in gliomas. *Lab. Invest.*, **88**, 910–925.
29. Jia,D., Jurkowska,R.Z., Zhang,X., Jeltsch,A. and Cheng,X. (2007) Structure of Dnmt3a bound to Dnmt3L suggests a model for *de novo* DNA methylation. *Nature*, **449**, 248–251.
30. Qiu,C., Sawada,K., Zhang,X. and Cheng,X. (2002) The PWWP domain of mammalian DNA methyltransferase Dnmt3b defines a new family of DNA-binding folds. *Nature Struct. Biol.*, **9**, 217–224.
31. Chen,T., Tsujimoto,N. and Li,E. (2004) The PWWP domain of Dnmt3a and Dnmt3b is required for directing DNA methylation to the major satellite repeats at pericentric heterochromatin. *Mol. Cell. Biol.*, **24**, 9048–9058.
32. Fuks,F., Hurd,P.J., Deplus,R. and Kouzarides,T. (2003) The DNA methyltransferases associate with HP1 and SUV39H1 histone methyltransferase. *Nucleic Acids Res.*, **31**, 2305–2312.
33. Tost,J. and Gut,I.G. (2007) DNA methylation analysis by pyrosequencing. *Nat. Protoc.*, **2**, 2265–2275.
34. Holz-Schietinger,C. and Reich,N.O. (2010) The inherent processivity of the human de novo DNA methyltransferase 3A (DNMT3A) is enhanced by DNMT3L. *J. Biol. Chem.*, **285**, 29091–29100.
35. Lister,R., Pelizzola,M., Dowen,R.H., Hawkins,R.D., Hon,G., Tonti-Filippini,J., Nery,J.R., Lee,L., Ye,Z., Ngo,Q.-M. *et al.* (2009) Human DNA methylomes at base resolution show widespread epigenomic differences. *Nature*, **462**, 315–322.
36. Gowher,H., Liebert,K., Hermann,A., Xu,G. and Jeltsch,A. (2005) Mechanism of stimulation of catalytic activity of Dnmt3a and Dnmt3b DNA-(cytosine-C5)-methyltransferases by Dnmt3L. *J. Biol. Chem.*, **280**, 13341–13348.
37. Fatemi,M., Hermann,A., Pradhan,S. and Jeltsch,A. (2001) The activity of the murine DNA methyltransferase Dnmt1 is controlled by interaction of the catalytic domain with the N-terminal part of the enzyme leading to an allosteric activation of the enzyme after binding to methylated DNA. *J. Mol. Biol.*, **309**, 1189–1199.
38. Jurkowska,R.Z., Anspach,N., Urbanke,C., Jia,D., Reinhardt,R., Nellen,W., Cheng,X. and Jeltsch,A. (2008) Formation of nucleoprotein filaments by mammalian DNA methyltransferase Dnmt3a in complex with regulator Dnmt3L. *Nucleic Acids Res.*, **36**, 6656–6663.
39. Dhayalan,A., Rajavelu,A., Rathert,P., Tamas,R., Jurkowska,R.Z., Ragozin,S. and Jeltsch,A. (2010) The Dnmt3a PWWP domain reads histone 3 lysine 36 trimethylation and guides DNA methylation. *J. Biol. Chem.*, **285**, 26114–26120.
40. Watanabe,D., Suetake,I., Tada,T. and Tajima,S. (2002) Stage- and cell-specific expression of Dnmt3a and Dnmt3b during embryogenesis. *Mech. Dev.*, **118**, 187–190.

41. La Salle,S., Mertineit,C., Taketo,T., Moens,P.B., Bestor,T.H. and Trasler,J.M. (2004) Windows for sex-specific methylation marked by DNA methyltransferase expression profiles in mouse germ cells. *Dev. Biol.*, **268**, 403–415.
42. Bourc'his,D., Xu,G.-L., Lin,C.-S., Bollman,B. and Bestor,T.H. (2001) Dnmt3L and the establishment of maternal genomic imprints. *Science*, **294**, 2536–2539.
43. Bourc'his,D. and Bestor,T.H. (2004) Meiotic catastrophe and retrotransposon reactivation in male germ cells lacking Dnmt3L. *Nature*, **432**, 96–99.
44. Kaneda,M., Okano,M., Hata,K., Sado,T., Tsujimoto,N., Li,E. and Sasaki,H. (2004) Essential role for *de novo* DNA methyltransferase Dnmt3a in paternal and maternal imprinting. *Nature*, **429**, 900–903.
45. Wienholz,B.L., Kareta,M.S., Moarefi,A.H., Gordon,C.A., Ginno,P.A. and Chedin,F. (2010) DNMT3L modulates significant and distinct flanking sequence preference for DNA methylation by DNMT3A and DNMT3B *in vivo*. *PLoS Genet.*, **6**, e1001106.
46. Suetake,I., Shinozaki,F., Miyagawa,J., Takeshima,H. and Tajima,S. (2004) DNMT3L stimulates the DNA methylation activity of Dnmt3a and Dnmt3b through direct interaction. *J. Biol. Chem.*, **279**, 27816–27823.
47. Purdy,M.M., Holz-Schietinger,C. and Reich,N.O. (2010) Identification of a second DNA binding site in human DNA methyltransferase 3A by substrate inhibition and domain deletion. *Arch. Biochem. Biophys.*, **498**, 13–22.
48. Ueda,Y., Okano,M., Williams,C., Chen,T., Georgopoulos,K. and Li,E. (2006) Roles for Dnmt3b in mammalian development: a mouse model for the ICF syndrome. *Development*, **133**, 1183–1192.